university of groningen

faculty of science and engineering

University of Groningen

Soft Limit of the 6-point Multi-DBI Double Copy Amplitude

MSc. Research Project

Written by Olivier Gelling at University of Groningen under the supervision of

Prof. dr. Diederik Roest and

Prof. dr. Anupam Mazumdar

August 26, 2022

Abstract

In this thesis we will attempt to reconstruct the 6-point DBI amplitude through the Double Copy method and probe it using soft limits. This specific example is chosen because DBI is both a Nambu-Goldstone boson and an exceptional Effective Field Theory, meaning it has unique soft limit cancellation properties. The relevant theoretical groundwork are explained and simplified examples of both traditional Feynman and Double Copy amplitudes are constructed in order to showcase their workings. Along with this we present some discussions of the soft limit, enhanced soft degrees, and some noteworthy examples relevant to the fields of soft limits, the Double Copy, and Nambu-Goldstone bosons. A fully usable Double Copy amplitude is not found due to the result containing many terms with forbidden factorisation. However, momentum space sample sets are taken to confirm that it should indeed factorise correctly. We will present the particular terms that constitute the soft cancellation of DBI's 6-point interaction found through Feynman and will discuss the way these can be interpreted in the DC amplitude. Potential similarities and discrepancies are presented and certain implications of those are discussed. Among these is the notion that one might be able to further constrain numerator terms constituting the Double Copy method by drawing a potential connection from the equivalence of the 4-point Feynman contact and Double Copy half-ladder diagrams to the 6-point Feynman exchange and Double Copy half-ladder diagrams.

Contents

1 Introduction

For quite some time field theory calculations have been done using path integrals, correlators, and Feynman diagrams and rules. These methods are straightforward and simple for some calculations, tough but doable for others, and incredibly complicated and time consuming for yet more. A stir was created when it was found that amplitudes can be reconstructed through relatively simple means: The Double Copy [1]. The Double copy was found to allow for a simple approach to complex amplitude calculations, like that of the rather complicated infinite-loop-correction calculation needed for gravity amplitudes, which could be recreated using–significantly more simple– Yang-Mills amplitudes. It was then found that one could copy many different amplitudes by taking a doublet of Jacobi relation-obeying numerator terms accompanying a new trivalent diagrammatic structure central to this new method.

As this is still a rather new find we have yet to understand much of the workings behind the Double Copy. For this exact reason we have set out to reconcile the Feynman and Double Copy amplitudes of a scalar theory with a particularly interesting behaviour in the Soft Limit of its 6-point interaction amplitude, namely Multi-DBI, in order to see if the unique destructive interference that occurs between the different contributions of its (in Feynman formalism) contact and exchange contributions is mimicked by the Double Copy half-ladder and snowflake contributions.

When one calculates the amplitude of (multi) DBI's 6-point interaction and then applies the soft limit to them, one will find the furious feat that these diagrams show a lower order soft degree than the overall amplitude. This is the result of the fact that the terms exhibiting this lower soft degree will cancel each other out once the full amplitude is taken. This phenomenon is rather unique in field theory. This fact exactly is why we will be attempting to find the same amplitude through the Double Copy, so we may they analyse the way these same terms come to cancel.

In part I of this thesis we will present the relevant topics needed to give full context to the task we have set out for ourselves. This will contain examples of how to calculate the Feynman and Double Copy amplitude of DBI in 4-point, an examination of the soft limit and how a theory's soft degree follows from its internal shift symmetry, and how enhanced soft degrees are established. We will present a couple of interesting and relevant examples of scalar theories connected to real particles, like the non-linear sigma model as a representation of light pions, and will shortly consider certain soft theorems of various levels of prestige.

In part II we first present our 6-point amplitude calculations through Feynman formalism, and use it to pinpoint exactly what is happening with the cancellation of terms between different Feynman diagrams in the soft limit. We will then present our findings for the Double Copy, which will sadly not be functionally usable. We then discuss what we can interpret from these results we found and how the soft cancellation of amplitude terms might be recovered in this new formalism. We will present some possible avenues of further study with respect to constraining the Double Copy's ansatze numerators further and ponder on the possibility of potential connections one can draw between then types of diagrams of the different approaches to constructing the amplitude.

Part I: Context and Theory

2 QFT Cliffnotes, Constructing an Amplitude

In this work we will be looking at the soft limit of Multi-DBI's 6-point interaction. As such it is of great importance to ground this discussion in the very foundations of amplitude calculations: QFT and Feynman formalism, including short discussions on flavour, and Mandelstam variables. After that we can move on to the more specialised pieces of this puzzle.

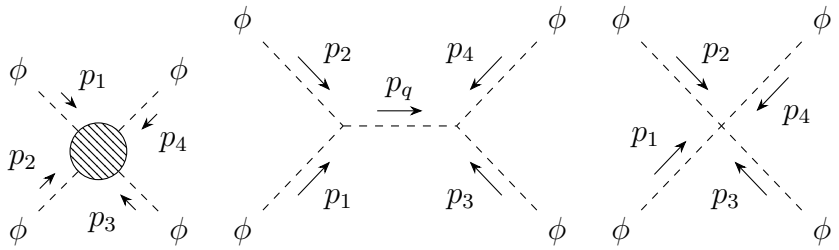

(a) Unspecified (b) Exchange (c) Contact

Figure 1: Unspecified, exchange, and contact diagrams

2.1 Feynman Diagrams and Amplitudes

Field Theory calculations are most commonly done through the Feynman approach where one uses a theory's Lagrangian to draw diagrams of an interaction one wishes to evaluate, which can then be used to derive a mathematical equation that expresses the desired amplitude using Feynman rules. This is a common short-cut often preferred over calculating such an interaction from the ground up, as one can use prior knowledge about the terms picked up from the structure of said diagram to construct the resulting amplitude. it is far easier to use 'plug-and-play' vertex rules and propagator terms than it is to go through the whole calculation over and over. To illustrate this process we will go through the relevant steps of applying Feynman rules to diagrams in a few simplified examples. As it serves as a useful example we shall take a generic 4-point self-interaction of a massless scalar theory, and pretend that there is a 3-point scalar interaction term to mimic the contribution of exchange diagrams.

A Lagrangian will have a subset of terms that make up its interactive part. We call this, unsurprisingly, the 'interaction Lagrangian'. These terms govern which vertices are permitted in interactions concerning the theory in question. We will be constructing a 4-point interaction. Thus, if the theory has 3-point vertices in its interaction Lagrangian then exchange diagrams are possible, and if it has a 4-point vertex then the contact diagram is relevant. If it has both then, naturally, both are. These exchange and contact diagrams are shown in Figure 1b and c. There are of course options to make more complicated diagrams, but these tend to be suppressed by their own coupling constants, and will generally not be of relevance. The two types of diagrams that we consider are "tree-level" diagrams, which means they are relatively simple and do not contain loops. This class of diagrams is often the main point of focus due to its contributions being the main–in other words: least suppressed–factors in an interaction's behaviour.

As one can see, the contact diagram has one vertex, while the exchange diagram has two, and a particle being exchanged between them; hence the name. When evaluating these diagrams' contributions to the 4-point interaction's amplitude we can plug in the vertex rules and propagator terms we know from Feynman diagram formalism. For the exchange diagram this will lead to the vertex rule being applied twice, alongside a propagator term arising from the exchange particle, with the momentum of said particle generating a pole in the term. External particles can be 'amputated' and thus do not need to be taken into account.

$$A_{exchange} \sim [\text{Vertex rule}] \times [\text{propagator term}] \times [\text{vertex rule}]$$

The contact diagram has no internal particle being exchanged, thus no propagator term is added, and only one vertex rule needs to be applied:

$$A_{contact} \sim [\text{Vertex rule}].$$

The propagator term is defined as:

$$D = \frac{i}{p^2 - m^2 + i\epsilon}$$

where p is the exchange momentum, in this case $p_1 + p_2$. m is the mass of the particles, which we have of course chosen to be 0, as our demonstrative scalar field might as well be rather similar to the one we will be using later on. This term can lead to a pole appearing in the amplitude, which is why $i\varepsilon$ is added, as it is a mathematical tool for contour integration, which can be used to get around singularities in integrals. We will not have need of it however.

These vertex rules and propagator terms come with some defined structure which can be read off of the Lagrangian and is expressed in momenta and coupling constants. Here we present two interaction Lagrangians to help us prepare for the ones we will need later on. We will use one three-point term to present and explore the nature of exchange diagrams in a simple and pedagogic fashion and a 4-point interaction term from DBI itself, as it is simple enough to use as an example and will be useful later on.

$$\mathcal{L}_i^3 = \kappa\phi\phi\phi \tag{1}$$
$$\mathcal{L}_i^4 = \lambda(\partial_\mu\phi)(\partial^\mu\phi)(\partial_\nu\phi)(\partial^\nu\phi) \tag{2}$$

We have not given the 3-point term derivatives as it makes for a nice and straight-forward example this way.

The 6-point DBI amplitude won't be this simple of course, but since this is merely a vehicle to discuss the methodology around Feynman amplitudes we have chosen to use an overly simplified term for the exchange diagram. One might envision this example as the scalar analogue of Yang-Mills theory.

To find all the relevant contributions to the ϕ^4 amplitude of our simplified theories we first remember that any loop contributions will be insignificant compared to the tree level 4-point contribution, and thus can be ignored, as is the same for higher order interactions usually. We will assume that κ and λ are of comparable scale. As we will see later on for DBI the different relevant vertices will scale in a similar way that these will if we set $\lambda = \kappa^2$. This, as we will see shortly, puts the two types of diagrams nicely on the same level.

We must now analyse the ways in which the diagrams can be permuted. The 4-point interaction can be envisioned like shown in Figure 1. The grey blob is quite simply a stand-in for "anything that can happen," which we of course amend to "anything that can happen and nets us a contribution worth looking at." Hence we get the classic three inequivalent channels: s, t, and u, from taking all inequivalent combinations of tying the external legs to the different vertices of the exchange diagram. for the 4-point term we get only the single contact diagram.

We now use a bit of intuition (and a lot of legwork done by others) to project Feynman rules onto these diagrams. For our cubic term this means the vertices contribute a factor

$$-i\kappa, \tag{3}$$

since no derivatives are found in that part of the interaction Lagrangian. The quartic term gives us:

$$-i\lambda(p_a \cdot p_b)(p_c \cdot p_d), \tag{4}$$

where a, b, c, and d denote the momentum of different legs of the interaction. These momentum dot products are the result of a Fourier transformation to the momentum domain of the field operators used to calculate the amplitude, where derivatives of fields bring one instance of that field's momentum down from the field operator's exponent within the correlator. The answer we find is then projected back onto the diagram to be able to consistently assign these Feynman rules to vertices and propagators without having to do the whole calculation over and over again–or at all in our case.

It is important to note here that even though the 4-point contact diagram has no channels it still has all the different permutations one can make with 4 fields, as the interaction term itself does not specify which leg enters into which ϕ. This means we have $4! = 24$ different contributions for the contact diagram, coming from all the ways we can combine the momenta in pairs. The same would go for the exchange diagrams, although since these hypothetical 3-point vertices have no partial derivatives the contribution need only be multiplied by a simple symmetry factor that arises from these different permutations, as they all contribute the same structure to the amplitude.

The last thing we have to take care of is the propagator. DBI contains only massless particles thus we will take our theory to have the same. The propagator will then be given by:

$$D = \frac{i}{q^2 + i\epsilon}, \tag{5}$$

where q^2 is the momentum exchanged between the vertices, which is determined by the topology of each specific diagram.

2.2 Mandelstam variables and Momentum Conservation

As shown above the amplitudes we are calculating are expressed in inner products of 4-momenta: $p_a \cdot p_b$. In a bit we will introduce flavour contractions, $t_{a,b}$ as well, as those are very integral to Multi-DBI, but for now let's stick with what we have. We can simplify our pairs of momenta into single entities, as their dot products link them together quite tightly: $p_a \cdot p_b \sim s_{a,b}$. It is important to stop and consider these variables for a moment. What we have just presented are Mandelstam variables, and they will be a very useful tool in expressing our amplitude.

Mandelstam variables, like momenta themselves, obey all applicable momentum conservation relations and on-shell conditions. The s channel we have presented above carries momentum $p_1 + p_2$ from one vertex to the other, its propagator mediates this process, and since we consider these interactions to be elastic no energy is lost. This means that $p_1 + p_2 = -p_3 - p_4$, where the minus sign is a result of taking all external momenta to be pointing towards their respective vertex. We can now take the norm of this equation: $(p_1 + p_2)^2 = (p_3 + p_4)^2$, which, when written out shows us that:

$$\begin{aligned}(p_1 + p_2)^2 &= p_1^2 + 2p_1p_2 + p_2^2 = 2p_1p_2 = s_{1,2}\\ (p_3 + p_4)^2 &= p_3^2 + 2p_3p_4 + p_4^2 = 2p_3p_4 = s_{3,4}.\end{aligned}$$

Which in simpler terms means that $s_{1,2} = s_{3,4}$. The same of course counts for the other channels: $s_{1,3} = s_{2,4}$ and $s_{2,3} = s_{1,4}$. All these follow from the information derived from kinematic relations provided by the exchange channels, and the fact that external particles, that being any of the numerically labelled ones, are on-shell. This means that their 4-momentum squared with itself equals 0, since p^2 returns the rest-mass of a particle and these particles are massless.

The contribution to this interaction by the three channels can now be constructed as follows:

$$-6i\kappa^2(\frac{1}{s_{1,2}} + \frac{1}{s_{1,3}} + \frac{1}{s_{2,3}})$$

and that of the contact diagram by:

$$\frac{-i\lambda}{4}(s_{1,2}s_{3,4} + perms) = -i2\lambda(s_{1,2}^2 + s_{1,3}^2 + s_{2,3}^2)$$

Where we have once again used the equivalence of 'opposite' Mandelstam variables, and the on-shell condition of external particles. We would like to point attention to the fact that only three Mandelstam variables are of note in our contributions: $s_{1,2}$, $s_{1,3}$, and $s_{2,3}$, even though there are 6 Mandelstam variables possible with our 4 external legs, namely:

$$s_{1,2},\ s_{1,3},\ s_{1,4},\ s_{2,3},\ s_{2,4},\ s_{3,4}.$$

The reason for this is of course the conservation laws we used above. There is, however, even more we can constrain. Using the on-shell condition and the fact that one of the external legs can always be taken as the sum of all others we find:

$$\begin{aligned}p_4 &= -(p_1 + p_2 + p_3)\\ p_4^2 &= 0\\ (p_1 + p_2 + p_3)^2 &= 0\\ s_{1,2} + s_{1,3} + s_{2,3} &= 0\end{aligned}$$

Where we then discover one final constraint:

$$s_{2,3} = -s_{1,2} - s_{1,3} \tag{6}$$

which shows us that there are in fact only two independent Mandelstam variables at play in this 4-point interaction. This leaves us with the following contact contribution:

$$A_4^{contact} = -i2\lambda(s_{1,2}^2 + s_{1,3}^2 + s_{2,3}^2) = -i4\lambda(s_{1,2}^2 + s_{1,3}s_{1,2} + s_{1,3}^2)$$

A point we must shortly discuss is lack of a factor 2 in the Mandelstam variables. In the chapters following this one we will use the simple equivalence of $p_a \cdot p_b = s_{a,b}$. This is not technically true, but it is not needed to take this detail into account. This numerical factor will be left out in most steps of the computation as the structure of the momenta (and flavour) is what matters far more than overall scalar values. This factor of $\frac{1}{2}$ will end up contributing very little to what we are looking for, as we are interested in the interplay of different interaction diagrams, rather than the overall amplitude. Since the contributions from both types of amplitudes have the same power of Mandelstam variables we incur no harm to our calculation by leaving this factor out.

Now, before we move on we must of course point out that the two contributions of our different interaction diagrams don't coincide on their units, as one has 4 powers of momentum, and the other has negative 2. This is of course the result of us, on purely pedagogical grounds, deciding that a 3-point scalar vertex suddenly exists. From here on out we will only consider the 4-point vertex as it actually fits DBI.

2.3 Flavour

Now that we have the steps for finding an amplitude set out for ourselves we can start complicating it by adding a last crucial property that our Lagrangian could be laden with: Flavour.

Flavour can be represented by a theory having an internal symmetry, like $O(N)$, $SO(N)$, $U(N)$, $SU(N)$, or something more complicated even. What this means is that a theory's particles come in different types, or in other words, the theory has particles of different 'flavours'. One theory having multiple, discernible, instances interacting with each other based on the same set of rules. A comparable example would be the colour of quarks, although quantum chromodynamics can be approximately expressed through the $SU(2)$ symmetry group, while Multi-DBI in the fundamental representation has an internal $SO(N)$ symmetry [2].

In a more palpable sense translating our theory to a multi-field theory is really as simple (or as complicated) as giving all the field operators a flavour index, and adding flavour contractions to the overall Lagrangian terms. We will demonstrate with the 4-point term of the example above, which we will now add $SO(N)$ flavour to, reflecting exactly what it will look like in Multi-DBI:

$$\mathcal{L}_4^{flav} = \lambda(\partial\phi^i \cdot \partial\phi^j)(\partial\phi^k \cdot \partial\phi^l)[\delta_{il}\delta_{jk} - \frac{1}{2}\delta_{ij}\delta_{kl}]$$

This addition will change the contribution of the contact term we presented above, gives us an amplitude with different flavour channels, all of which are the same under permutation, as is the nature of an internal symmetry like this. We now have our 4-point contribution:

$$\begin{aligned} A_4^{flav} \sim s_{1,2}^2 \left(-\frac{1}{2}t_{1,2}t_{3,4} + \frac{1}{2}t_{1,3}t_{2,4} + \frac{1}{2}t_{1,4}t_{2,3}\right) \\ + s_{1,3}^2 \left(\frac{1}{2}t_{1,2}t_{3,4} - \frac{1}{2}t_{1,3}t_{2,4} + \frac{1}{2}t_{1,4}t_{2,3}\right) \\ + s_{2,3}^2 \left(\frac{1}{2}t_{1,2}t_{3,4} + \frac{1}{2}t_{1,3}t_{2,4} - \frac{1}{2}t_{1,4}t_{2,3}\right) \end{aligned}$$

Where we can separate the three different flavour channels, $t_{12}t_{34}$, $t_{13}t_{24}$, and $t_{14}t_{23}$, to obtain their individual amplitudes:

$$\begin{aligned} A_{12,34} &\sim \frac{1}{2}\left(-s_{1,2}^2+s_{1,3}^2+s_{2,3}^2\right) &&= s_{1,3}\left(s_{1,2}+s_{1,3}\right) &&= -s_{1,3}s_{2,3} \\ A_{13,24} &\sim \frac{1}{2}\left(s_{1,2}^2-s_{1,3}^2+s_{2,3}^2\right) &&= s_{1,2}\left(s_{1,2}+s_{1,3}\right) &&= -s_{1,2}s_{2,3} \\ A_{14,23} &\sim \frac{1}{2}\left(s_{1,2}^2+s_{1,3}^2-s_{2,3}^2\right) &&= -s_{1,2}s_{1,3}. \end{aligned}$$

It should be easily visible that these are indeed the same under permutation. We have now also directly presented multi-DBI's 4-point amplitude.

With this we have exhausted the 4-point example's usefulness to Feynman formalism, and shall thus move on to the centrepiece of this play: DBI Theory.

3 DBI

We hereby introduce the vehicle through which we will attempt to probe the Double Copy mechanism. DBI, which stands for Dirac Born Infeld, is a massless scalar theory. It is one of the well known embodiments of a Nambu-Goldstone boson, and as such has a lot of prior study to its name. It abides by an enhanced shift symmetry, which grants it special 'enhanced' behaviour in the soft limit, and is both an Effective Field Theory (EFT) *and* an *enhanced* EFT. On top of this DBI is also 'soft reconstructible', which means one can reconstruct it from soft assumptions [3] and it is one of the theories that abides by the Double Copy construction [1, 4, 5]. We will introduce it by itself here and expand on its soft behaviour later on in the Soft Limits chapter.

3.1 DBI Theory

DBI theory notes a scalar theory that has zero mass and only even interaction terms. The action of this theory can be derived from the description of a d-brane fluctuating in (d+1)-dimensional spacetime [4, 6].

A brane is what we call a hypersurface; a membrane with $d+1$ dimensions that we embed within a $D+1$ dimensional "bulk", or "hyperspace", spacetime. When doing this we can use a variety of embedding functions to describe the behaviour of the brane in that higher order spacetime, connecting coordinates on the brane itself, say x^μ, to coordinates in the hyperspace, say X^μ. This gives us embedding functions $X^A(x^\mu)$, with $A \in \{0,...,D\}$ and $x \in \{0,...,d\}$. These embedding functions are maps from the brane's topology to that of the bulk [6].

If this hyperspace is granted a metric, say $\mathcal{G}_{AB}$, the above embedding functions can be used to recover an induced metric in brane coordinates:

$$g_{\mu\nu}(x) = \frac{\partial X^A}{\partial x^\mu}\frac{\partial X^B}{\partial x^\nu}\mathcal{G}_{AB}(X)$$

The connection between both of these can be used to recover Riemann curvature tensors, bulk vectors, normal vectors, and extrinsic curvature tensors, all of which transform covariantly under diffeomorphis of both the brane and bulk. A covariant derivative, $\mathcal{D}_\mu$, exists on the brane which respects both of these transformations [6].

With all of the ingredients mentioned above one can then construct an invariant action, which describes the brane's dynamics, and a general form of it is given by:

$$S_{universal} \equiv -\int d^{d+1}x\sqrt{-g} = -\int d^{d+1}x\sqrt{-det(\partial_\mu X^A \partial_\nu X^B \mathcal{G}_{AB}(X))}. \tag{7}$$

This action allows us to recover DBI, which is found when taking the bulk spacetime to be flat, i.e. $D = d + 1$ and $\mathcal{G}_{AB} = \eta_{AB}$. Applying these conditions to the geometric ingredients presented above, along with fixing unitary gauge, allows us to reduce the universal brane action to [6]:

$$S_{DBI} \equiv -\int d^{d+1}x\sqrt{1 + (\partial\phi)^2}. \tag{8}$$

With $(\partial\phi)^2 = \eta_{\mu\nu}\partial^\mu\phi\partial^\nu\phi$. This action allows us to recover the DBI Lagrangian upon expanding the root, which we will consider without flavour for now [2, 6]:

$$\mathcal{L}_{\text{DBI}} = -\frac{1}{2}(\partial\phi)^2 + \frac{\lambda}{8}\Big[(\partial\phi)^2\Big]^2 - \frac{\lambda^2}{16}\Big[(\partial\phi)^2\Big]^3 + ... \tag{9}$$

where λ is the coupling constant that scales the interactions and the ellipsis imply other, higher order, terms that we will not need to bother with.

What we have here is a velocity term, $\frac{1}{2}(\partial\phi)^2$, a quartic interaction term, $[(\partial\phi)^2]^2$ that scales with λ, and a sextic interaction term, $[(\partial\phi)^2]^3$, which scales with λ^2. There are an infinite amount of even interaction terms (8, 10, 12, etc) resulting from the root's expansion, but those fall off very fast due to suppression by the higher powers of λ and are thus again not relevant to lower order tree-level diagrams, and with it to what we are interested in.

The multi-field generalisation of this theory, which we will be working with, arises from the symmetry breaking pattern [2]:

$$\frac{ISO(d+N)}{SO(d)\times SO(N)}, \tag{10}$$

with d again the spacetime dimension (including time already) and N that of the flavour's $SO(N)$ symmetry mentioned above.

DBI is invariant under a a (d+1)-dimensional Lorentz symmetry, and the following shift symmetry [2, 4, 6]:

$$\delta_{DBI}\phi(x) = c + b^\mu(x_\mu + \phi\partial_\mu\phi) \tag{11}$$

Where c is a scalar and i and j are flavour indices, the effect of which which we will consider later on in this chapter. This shift has both a constant and linear space-time component, and is quadratic in the field ϕ itself. We will dig into the implications of this shift symmetry towards the theory's soft behaviour in the soft limit chapter, but that is not the only thing this shift symmetry brings about.

When a degenerate ground state, like for instance the well known $U(1)$ mexican hat potential, is introduced to a theory with a symmetry like this we encounter spontaneous symmetry breaking (SSB). This is a phenomenon introduced by Yoichiro Nambu in 1960; expanded upon by, among others, Jeffrey Goldstone; and applied in many different ways since. The Higgs mechanism is one of many things that resulted from this initial idea of SSB. A broken symmetry like we see here gives rise to a Nambu-Goldstone boson. Since this shift symmetry suffers the same fate DBI is one of these.

DBI does not stand on its own, as it is part of a triplet of enhanced EFTs with many internal connections. The other two members of this triplet are the Special Galileon (SG) and the Non-Linear Sigma Model (NLSM). All three of these are NGBs, and can even be shown to map into one another under certain flavour-derivative transformations [7]. Moreover, NLSM has been shown to be an excellent representation of light pions.

3.2 The 6-Point Interaction

We will be studying the DBI field's 6-point self-interaction, where we take 3 particles to come in and 3 to go out of an unspecified interaction. This interaction is governed mainly by two types of diagrams, those being contact and exchange, as we will again consider loop corrections to be too suppressed to matter to us. We will discuss the diagrams that make up this interaction, present their (Single) DBI Feynman rules and discuss the momentum conservation laws at play. Once that is done we will translate what we have to Multi-DBI by adding flavour, much like we did in last chapter's example.

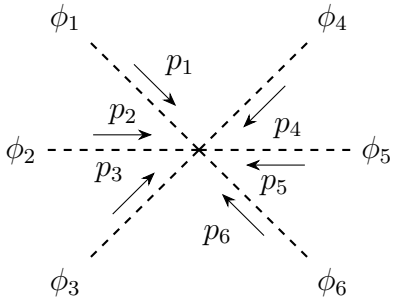

Figure 2: 6-point DBI contact diagram

3.2.1 Contact

The contact diagram is shown in Figure 2 and is represented in the Lagrangian (9) by the term:

$$\mathcal{L}_6 = \frac{\lambda^2}{16}\Big[(\partial\phi)^2\Big]^3. \tag{12}$$

As shown in our simplified example above the partial amplitude of a diagram can be found by applying the relevant Feynman rules to its structure. The Feynman rule for this vertex is similar to the one found in the previous section as well, except for an added set of legs. We must again remind ourselves that the vertex term does not specify which leg goes where, meaning we need to take all different combinations with which we can place the external legs into the vertex:

$$-i\frac{\lambda^2}{16}\sum_{perms}(p_a\cdot p_b)(p_c\cdot p_d)(p_e\cdot p_f) \tag{13}$$

As one can see, the three square sets of $\partial\phi$'s give three products of momentum, which multiply the regular vertex rule coming from the coupling constant together with a factor $-i$.

To use this vertex term one must plug in all possible permutations of the leg orientations, which means distributing $6! = 720$ configurations over term (12). This isn't much of an

issue for now as the terms remain relatively simple but will come in to play far more abundantly once flavour is being factored in.

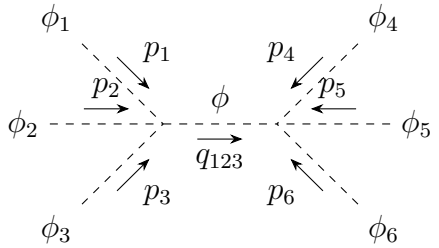

Figure 3: 6-point DBI exchange diagram

3.2.2 Exchange

The other type of tree-level diagrams possible for this interaction is the exchange diagram. These consist of two 4-point vertices and a propagator running between them, as is shown in Figure 3. The external legs will be tied to the vertices in whichever way possible that doesn't create degenerate diagrams. This can be done in (remembering basic statistics) $6!\,/(3!\,(6-3)!\,) = 20$ different ways. Half of these, however, are equivalent to the others due to momentum conservation, so we end up with only 10 that we need to take into account. The most straightforward example of an exchange diagram can be seen in Figure 3, and some of the more complicated ones are shown in Figure 4.

Similarly to the contact diagram the vertices don't specify which leg goes where, so we have $4! = 24$ permutations of momenta for each vertex, which gives us $24 \times 24 = 576$ terms to consider for every exchange diagram.

The vertices of these diagrams are governed by the Lagrangian's quartic term:

$$\mathcal{L}_6 = \frac{\lambda}{8}\Big[(\partial\phi)^2\Big]^2, \tag{14}$$

which then gives us the vertex rule as follows:

$$-\frac{i\lambda}{8}\sum_{perms}(p_a \cdot p_b)(p_c \cdot p_{q_{abc}}) \tag{15}$$

where q_{abc} of course is the exchanged momentum.

The other needed Feynman rule here is the one describing the propagator, which is given as follows:

$$D_{q_{a,b,c}} = \frac{i}{s_{a,b,c}}, \tag{16}$$

where we neglect the $i\epsilon$ prescription already, as we will not make use of it.

To construct the amplitude of an exchange diagram we, like before, will have to apply the vertex rule to both vertices and then add the propagator term inbetween. Before we do so, however, we will once again discuss the momentum conservation rules relevant to this interaction.

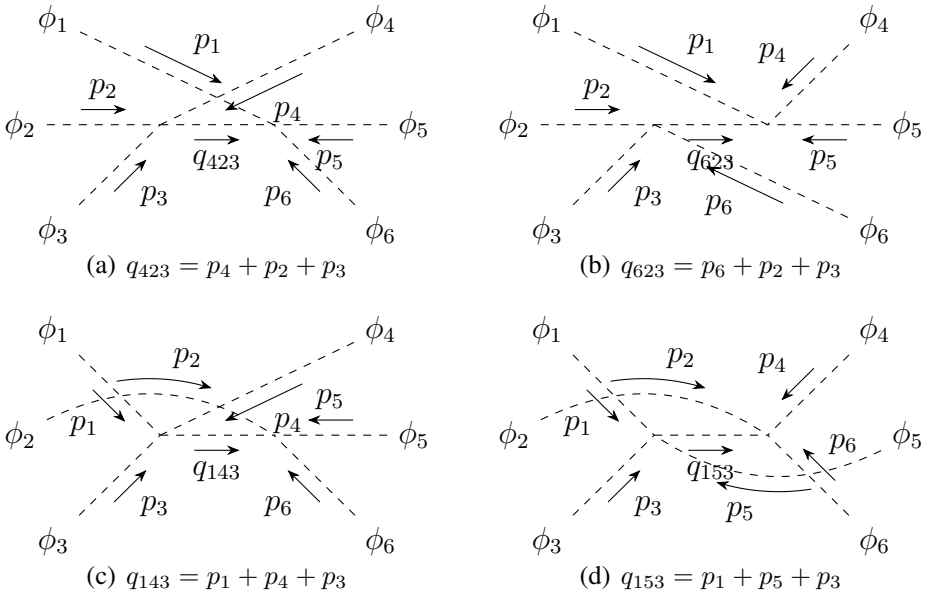

(a) $q_{423} = p_4 + p_2 + p_3$ (b) $q_{623} = p_6 + p_2 + p_3$

(c) $q_{143} = p_1 + p_4 + p_3$ (d) $q_{153} = p_1 + p_5 + p_3$

Figure 4: Some exchange diagrams

3.3 Momentum Conservation

To work out our amplitudes in full it is important to establish the way momentum conservation guides this interaction. We know of course that the total momentum is conserved just like with the 4-point example, giving us equalities like the following:

$$s_{1,2,3} = s_{4,5,6}, \tag{17}$$

and all its permutations, where $s_{a,b,c} = s_{a,b} + s_{a,c} + s_{b,c}$. We also, again, must consider the fact that one of our external legs can be taken as the sum of all other momenta:

$$p_6 = -(p_1 + p_2 + p_3 + p_4 + p_5), \tag{18}$$

where the signs were chosen such that all momenta point towards the interaction, which was done for mathematical simplicity. This condition in turn gives us a similar constraint as we saw above when applying the on-shell condition to this leg:

$$p_1 \cdot p_2 + p_1 \cdot p_3 + p_1 \cdot p_4 + p_1 \cdot p_5 + p_2 \cdot p_3 + p_2 \cdot p_4 + p_2 \cdot p_5 + p_3 \cdot p_4 + p_3 \cdot p_5 + p_4 \cdot p_5 = 0, \tag{19}$$

where on-shell conditions apply to all external legs. This can be written out far more nicely in our Mandelstam variable notation:

$$s_{1,2} + s_{1,3} + s_{1,4} + s_{1,5} + s_{2,3} + s_{2,4} + s_{2,5} + s_{3,4} + s_{3,5} + s_{4,5} = 0. \tag{20}$$

granting us another equation that allows us to express one of these variables as the sum of the others.

Altogether then we have 10 constraint equations from all the equivalent exchange channels, which, when solved, constrain 5 Mandelstam variables, and the on-shell condition of p_6^2, which gives one last constraint. In the results we will work primarily with the initial constraints expressing every Mandelstam variable that contains a value of p_6 as a sum of others, and will then add a last one picking from those left as we please. We end up choosing $s_{2,5}$ simply because it made the result fit nicely in Mathematica.

3.4 Feynman Rules to Amplitudes

Going from the contact diagrams and the relevant vertex rule to a partial amplitude is relatively straightforward, as the diagram needs only the single Feynman rule (and all its permutations) to be turned into a bona fide (partial) amplitude. The exchange diagrams, however, need a little more work to be ready for use. Accounting for all the different relevant diagrams and combining the rules for both vertices and the propagator, *and* accounting for the different permutations of the momenta going into each vertex we end up with the exchange amplitude expressed as follows:

$$\mathcal{A}^{partial}_{exchange} = \left(\frac{\lambda}{8}\right)^2 \sum_{diagrams} \frac{i}{s_{q_{abc}}} \Big[\sum_{perms} (p_a \cdot p_b)(p_c \cdot p_{q_{abc}}) \Big] \Big[\sum_{perms} (p_d \cdot p_e)(p_f \cdot p_{q_{abc}}) \Big] \quad (21)$$

where q_{abc} represents the exchange momentum. a, b, c and d, e, f are the incoming and outgoing momenta respectively. These are, as before, a result of the different ways the partial derivatives can connect the legs through dot products, and the sum over q_{abc} gives us all the different channel topologies. Presenting this in Mandelstam variables would only make sense after substituting the exchange momentum, which will not add much of worth to our explanation right now while making the formula a bit lengthier than needed, thus we will leave this term as-is.

The contact contribution can however be presented in Mandelstam variables quite easily:

$$\mathcal{A}^{partial}_{contact} = -i\frac{\lambda^2}{16} \sum_{perms} s_{a,b} s_{c,d} s_{e,f} \quad (22)$$

Now that we *finally* have all of these pieces set up it's time to give them a nice coat of paint, although that joke would probably work better had we been about to introduce colour charge to our theory.

3.5 Multi-DBI

Multi-DBI is essentially an extension of DBI. The fields ($\partial\phi$) will henceforth carry a flavour index, which means they obey an internal SO(N) symmetry. The interaction terms relevant to this variation of DBI are similar to the ones we saw before but of course with flavour information added. We thus get

$$\mathcal{L}_6 = \lambda^2 (\partial_\mu \phi^i)(\partial^\mu \phi^j)(\partial_\nu \phi^k)(\partial^\nu \phi^l)(\partial_\rho \phi^m)(\partial^\rho \phi^n) \Big[\frac{1}{6}\delta^{in}\delta^{jk}\delta^{lm} - \frac{1}{8}\delta^{ij}\delta^{km}\delta^{ln} + \frac{1}{48}\delta^{ij}\delta^{kl}\delta^{mn} \Big] \quad (23)$$

for the contact diagram, and

$$\mathcal{L}_4 = \frac{\lambda}{4} (\partial_\mu \phi^i)(\partial^\mu \phi^j)(\partial_\nu \phi^k)(\partial^\nu \phi^l) \Big[\delta^{il}\delta^{jk} - \frac{1}{2}\delta^{ij}\delta^{kl} \Big] \quad (24)$$

for the vertices that will constitute the exchange diagrams. Apart from the addition of flavour indices i, j, k, l, m and n, and flavour deltas to induce contraction structure, the numerical values weighing the terms have been slightly altered. Here we can see that the deltas, when applied to the fields, lead to terms where the flavour indices connect differently compared to the partial derivatives, adding a new level of structure to the theory, giving each vertex multiple terms with different flavour structures to governing its contribution. Luckily for us the propagator remains unchanged.

These updated interaction terms now allow us to construct flavour-full vertex rules from which we can find the partial amplitudes. We will skip presenting the vertex and propagator rules again, as it should be clear by now how these work, and will instead present the formulas describing the partial amplitudes right away:

$$\mathcal{A}^{flavour}_{contact} = -i\lambda^2 \sum_{perms} s_{a,b}s_{c,d}s_{e,f}\left(\frac{1}{6}\delta_{a,f}\delta_{b,c}\delta_{d,e} - \frac{1}{8}\delta_{a,b}\delta_{c,e}\delta_{d,f} + \frac{1}{48}\delta_{a,b}\delta_{c,d}\delta_{e,f}\right) \quad (25)$$

gives the contact diagram, where the flavour indices have been 'spent' and are now indicating which external legs are contracted with each other.

The exchange diagrams will, like before, be a bit more complicated:

$$\mathcal{A}^{flavour}_{exchange} = \left(\frac{\lambda}{4}\right)^2 \sum_{diagrams} \frac{i}{s_{q_{abc}}}\left(\sum_{perms}(p_a \cdot p_b)(p_c \cdot p_{q_{abc}})\right)\left(\delta_{a,q}\delta_{b,c} - \frac{1}{2}\delta_{a,b}\delta_{c,q}\right) \times \left(\sum_{perms}(p_d \cdot p_e)(p_f \cdot p_{q_{abc}})\right)\left(\delta_{q,f}\delta_{d,e} - \frac{1}{2}\delta_{q,d}\delta_{e,f}\right) \quad (26)$$

we once again run into the fact that substituting q for the full exchange momentum sum to be able to show the proper Mandelstam variable form would only serve to make the equation less comprehensible. Substituting the p_q terms will result in a sum of Mandelstam variables, after which the flavour contractions with qs in them will link together, like, for instance, $\delta_{a,q}\delta_{q,f} = \delta_{a,f}$. This makes sense of course, as the flavour of the exchange particle does not change inbetween the vertices, thus it is carried out of one vertex and into the other.

What we have here is an excellent template to feed into a Mathematica script, which can then do the rest of the calculation for us. Hence we can now consider the theory section regarding how to construct the Feynman amplitude to be concluded, and proceed onwards.

4 Double Copy

The Double Copy is a phenomenon found relatively recently, where complicated amplitudes, like that of gravity's self-interaction–which has an infinite amount of loop corrections and thus is quite computationally heavy–can be reconstructed through relatively simple means. One can multiply two specific numerator factors and divide them by a propagator term of sorts to recreate an amplitude. This was first done by recreating a gravity amplitude using the Yang-Mills interaction [1] as a template for the 'numerator terms'. This would only be the first of many theories that have been found to show a connection of this sort. Its implications, and how far its web of connected theories might reach, are not yet fully understood. As such it is currently a very active area of theoretical research.

4.1 Duality between Colour and Kinematics

The advent of the Double Copy was the result of the curious property that colour and kinematic factors of gauge theories, specifically Yang-Mills (YM) and gravity, obeyed Jacobi relations of their own. One can construct 4-point YM colour factors, $c_s, c_t,$ andc_u,

from the relevant structure constants, and 4-point gravity kinematic factors, n_s, n_t, andn_u, from momentum and polarisation vectors using well-known Feynman rules. These factors can then be shown to obey colour and kinematic Jacobi identities [1]:

$$c_s + c_t + c_u = -2(f^{a_1a_2b}f^{ba_3a_4} + f^{a_2a_3b}f^{ba_1a_4} + f^{a_3a_1b}f^{ba_2a_4}) = 0, \tag{27}$$

and

$$n_s + n_t + n_u = 0. \tag{28}$$

The colour relation is satisfied by the group theory structure constants (f^{abc} in a gauge theory, and the kinematic factors are found to neatly cancel out when the on-shell conditions are applied to them.

The equivalence between these colour and kinematic identities is what was then dubbed a "duality between colour and kinematics." It would later be found that this hidden structure that connects different theories stretches far beyond just YM and gravity.

The full implications of these analogous identities is also yet to be presented, as it was proposed that, through sharing the same Jacobi relations, these numerators might be mutually interchangeable. When one swaps colour factors for kinematic factors in the YM 4-point amplitude,

$$i\mathcal{A}_4^{tree} = g^2\left(\frac{n_s c_s}{s} + \frac{n_t c_t}{t} + \frac{n_y c_u}{u}\right) \rightarrow i\mathcal{M}_4^{tree} = \left(\frac{\kappa}{2}\right)^2\left(\frac{n_s^2}{s} + \frac{n_t^2}{t} + \frac{n_y^2}{u}\right), \tag{29}$$

(along with of course the coupling constants) a new, once again gauge-invariant, object is found. This new entity is moreover quite simply the 4-point gravity amplitude. The kinematic numerators are now 'doubled up', hence it was called the "double copy." The amplitude that is constructed here through this ad-hoc method was found to necessarily describe the scattering of four gravitons in Einstein's General Relativity, up to an overall normalisation, with multiple avenues of proof to boot[1]. The specific amplitude that we see reproduced here is the Kawai-Lewellen-Tye (KLT) form of the gravity amplitude [1, 8], which was initially derived in the low-energy limit of string theory.

With some extra mathematical steps, like substituting a chosen solution for one of the colour or kinematic factors into the YM amplitude and solving for the partial amplitudes that result, one can show the direct connection between both of these amplitudes:

$$\mathcal{M}_4^{tree}(1,2,3,4) = -isA_4^{tree}(1,2,3,4)A_4^{tree}(1,2,4,3), \tag{30}$$

with $A_4^{tree}(1,2,3,4)$ denoting a partial (YM) amplitude. This is exactly one of the KLT relations between gravity and gauge, which here has been recovered simply from colour-kinematics duality and gauge invariance constraints.

What this means is that we can reconstruct the 4-point gravity amplitude by using a far simpler theory, namely YM, and simply swapping out the relevant numerators. This phenomenon made certain complicated amplitude calculations significantly easier to do, and was furthermore found to connect a wide network of theories, one of which will be relevant to our research here. The full 'web' is presented in Figure 5 below, courtesy of the review article by the very pioneers of the Double Copy themselves. Among the connections are (of course) Einstein gravity and YM, but also EFTs like the Special Galileon, Dirac-Born-Infeld, Non-Linear Sigma Model–which once again form a nice little triplet- and many more that we know of right now, with potential for more to be added!

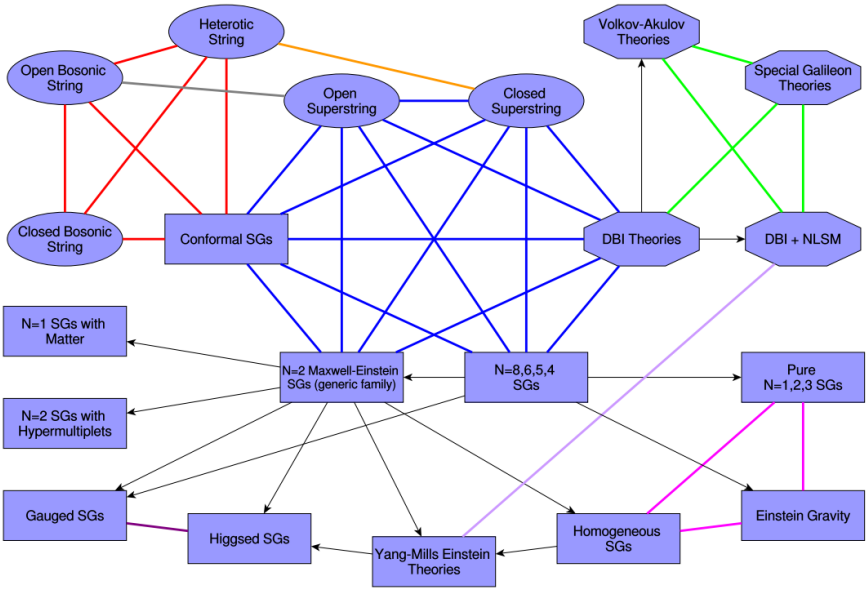

Figure 5: The web of Double Copy reconstructible theories [1].

4.2 Double Copy in action

To present the phenomenon in its most straight forward form we will go through the 4-point example for DBI, reconstructing it from numerators we generate from an ansatze approach. We start with the general formula that governs the DC phenomenon [1]:

$$\mathcal{A}_{\text{DC}} = i \sum_{j=1}^{\#BCJ} \frac{A_j B_j}{D_j}. \tag{31}$$

One multiplies two numerator factors, A_j and B_j, and divides them by the relevant Feynman propagator products, $\frac{1}{D_j}$, for all the relevant diagrams–hence the sum–to reconstruct an amplitude. The diagrams used to pick out the relevant propagator terms will not be those derived from the Lagrangian, and thus won't look like our Feynman diagrams. It was found [1] that trivalent graphs and the propagator structure that arises from those is what is needed to make this phenomenon fit, as there seems to be a way to, using th Jacobi identities, permutatively map interactions into only trivalent connections. This even supersedes the Lagrangian of a theory, meaning that a theory with only even vertices (like DBI) can still be represented with trivalent diagrams for the DC. These diagrams are dubbed BCJ diagrams, after the trio that found the DC phenomenon and constructed the diagrammatic approach needed for it: Zvi Bern, John Joseph Carrasco, and Henrik Johansson.

Which theory will be reconstructed depends on the types of numerators used. These numerators contain information pertaining to the theory in the form of kinematic and flavour factors. We will show a few examples to demonstrate the process. SG, Multi-DBI, and NLSM are considered to be enhanced EFTs due to properties relating to soft limits, and can be reconstructed through the use of equation 31. The numerator terms needed to do so are as follows in Table 1:

Theory	$A_j \times B_j$
SG	kinematic $\times$kinematic
DBI	kinematic $\times$flavour
NLSM	flavour $\times$flavour

Table 1: Effective Field Theory construction through the Double Copy

One can recover amplitudes of the Special Galileon theory by substituting kinematic numerators relevant to the specific diagram being calculated into A_j and B_j. One can instead find DBI using a kinematic and a flavour factor, and NLSM by using only flavour factors.

4.3 BCJ diagrams

When studying the relation between colour and kinematics, Bern, Carrasco, and Johansson found that one could "reorganise the perturbative expansion of tree-level amplitudes" by writing them out in exclusively cubic diagrams once their characteristic factors (colour or kinematic, or both) would obey analogues to the same Jacobi relation. We call the diagrams that are constructed from this 'BCJ diagrams', and they are at the very heart of the functioning of the Double Copy phenomenon.

Cubic diagrams, by their very nature, come in two forms, depending on how many external legs one considers. That is, tree-level ones do. Loops will make things more complicated, as they are wont to do, but can be, as expected, ignored. For any order diagram one can make 'half-ladder' shapes, lining up and connecting all the vertices, where each also connects to an external leg, shown in Figure 6a. With 6 or more external legs, however, one can also form 'snowflake' diagrams, as shown in Figure 6b. As the names indicate, the half-ladder diagrams look like a ladder with one side missing, and the snowflakes look like simple snowflakes.

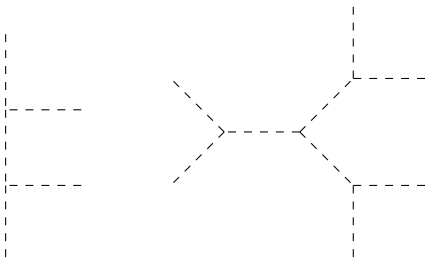

(a) Half-ladder (b) Snowflake

Figure 6: Half-ladder and Snowflake BCJ Diagrams

4.4 Propagators, Numerators, and Amplitudes

Now that we have most of the necessary information presented we can try to build our own DC amplitude. This will be particularly useful as the numerators can be somewhat tricky to present without context. It turns out that these factors arise from particular BCJ diagrams of theories, and as such finding them is a work of their own. We will be borrowing from prior work to skip finding these numerators and put them into practice directly. More information about them can be found in [2, 1]. They are constructed as a general ansatze which is then constrained to fit our needs. More on this process in a bit.

Taking 4-point Multi-DBI as our practice project will serve us well here. We will start off by finding the BCJ diagrams. As this interaction is below that which can start generating snowflake diagrams we have only the half-ladder topology to consider. This means that we get diagrams quite similar to our exchange diagrams presented above. The famous s, t, and u channels are in essence half-ladder diagrams already! Now we need to read off the propagators relevant to the diagrams and fill in the correct numerator terms.

To find the propagator terms we only have to look at the internal lines, like one does with Feynman diagrams, and multiply any of the propagator terms with each other. For our diagrams (Figure 7) that is simply $1/s_{ab}$ for each permutation of the external momenta, which one does by filling all combinations of 1, 2, 3, and 4 into a, b, c, and d. With that

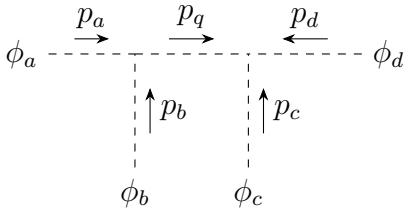

Figure 7: 4-point half-ladder BCJ diagram

done we must now find the numerator terms. As mentioned, this is a process of Ansatze and fine-tuning. It would be wise to present the DC equation (31) in its updated form, which represents the 4-point interaction we are working with specifically:

$$\mathcal{A}_{\text{DC}}^{\text{4-DBI}} = i \sum_{perms} \frac{N_{a,b,c,d} F_{a,b,c,d}}{s_{a,b}} \tag{32}$$

With $N_{a,b,c,d}$ the kinematic, and $F_{a,b,c,d}$ the flavour numerator.

One knows what the momentum scaling of a numerator term will have to be depending on the interaction considered, as we already know the answer we are working towards through Feynman formalism, and know how many powers of momentum we need to 'overshoot' to compensate for the propagator dividing them out. The same goes for flavour factors, although those don't require any overshoot of course. This means that for our example the total amount of Mandelstam variables we need from the numerators is 3, which will then be divided over the kinematic factor, which will supply 2 powers of Mandelstam variables, and the flavour factor, which will provide a Mandelstam variable and flavour contractions [2]. These factors can be used for SG, DBI, and NLSM without much further ado.

Starting with a general template of a weighted sum of each possible combination of Mandelstam variables for the kinematic numerator, and each combination of a Mandelstam variable and flavour terms for the flavour numerator, one demands these overall factors to obey their kinematic and flavour (previously colour) Jacobi relations to force most of the weighting constants to take on a specific value and thus giving the numerator term a defined shape. Then afterwards one restricts the result further to end up factorising correctly as well. What one will be left with, for the 4-point interaction at least, are the following numerator terms [2]:

$$N_{a,b,c,d} = \frac{1}{2} z_{1,2} s_{a,b} \left(s_{a,b} + 2 s_{b,c} \right) \tag{33}$$

$$F_{a,b,c,d} = s_{b,c}\left(\left(z_{3,1}-z_{3,2}\right)t_{a,d}t_{b,c} + \left(z_{3,1}-z_{3,2}\right)t_{a,c}t_{b,d} - 2z_{3,2}t_{a,b}t_{c,d}\right) + s_{a,b}\left(z_{3,1}t_{a,c}t_{b,d} - z_{3,2}\left(t_{a,d}t_{b,c}+t_{a,b}t_{c,d}\right)\right) \quad (34)$$

for the kinematic and flavour factors. It is important to note that in this representation we still have gauge parameters, which will have to be set to some value later on for the amplitude to match that of the Feynman approach.

Now that we have the numerators, know which propagator terms are needed, and know the diagrams we need to apply all these to we can do exactly that, finding the amplitude as follows:

$$\begin{aligned}\mathcal{A}_{\text{DC}}^{\text{4-DBI}} = -\frac{3}{2}z_{1,2}\Big(&s_{1,2}^2\left(2t_{1,3}t_{2,4}z_{3,2} + t_{1,4}t_{2,3}\left(z_{3,2}-z_{3,1}\right) + t_{1,2}t_{3,4}\left(z_{3,2}-z_{3,1}\right)\right)\\ &+ 2s_{1,3}s_{1,2}\left(\left(t_{1,3}t_{2,4}+t_{1,2}t_{3,4}\right)z_{3,2} - t_{1,4}t_{2,3}z_{3,1}\right)\\ &+ s_{1,3}^2\left(2t_{1,2}t_{3,4}z_{3,2} + t_{1,4}t_{2,3}\left(z_{3,2}-z_{3,1}\right) + t_{1,3}t_{2,4}\left(z_{3,2}-z_{3,1}\right)\right)\Big).\end{aligned} \quad (35)$$

Which is starting to amount to quite the line of contributions. We do notice however, that some of the gauge parameters line up very nicely, and can be cancelled out by choosing $z_{3,2} = z_{3,1}$ and $z_{1,2} = -1/(3z_{3,1})$, which gives us:

$$\mathcal{A}_{\text{DC}}^{\text{4-DBI}} = s_{1,2}^2 t_{1,3}t_{2,4} + s_{1,3}^2 t_{1,2}t_{3,4} - s_{1,3}s_{1,2}\left(t_{1,4}t_{2,3} - t_{1,3}t_{2,4} - t_{1,2}t_{3,4}\right) \quad (36)$$

This should start to look somewhat familiar, but to make it even easier to recognise we will pick out the three flavour channels:

$$\mathcal{A}_{12,34} = s_{1,3}\left(s_{1,2}+s_{1,3}\right) = -s_{1,3}s_{2,3} \quad (37)$$

$$\mathcal{A}_{13,24} = s_{1,2}\left(s_{1,2}+s_{1,3}\right) = -s_{1,2}s_{2,3} \quad (38)$$

$$\mathcal{A}_{14,23} = -s_{1,2}s_{1,3} \quad (39)$$

Which are indeed exactly the amplitudes we found through the Feynman approach.

4.5 The 6-point Interaction in DC

4.5.1 6-point BCJ Diagrams

As shown above, finding an amplitude with the DC can be quite different from the Feynman approach. This will become even more apparent for the 6-point interaction as the cubic vertices are here to stay, even for an interaction of this order. This means that we now have to consider snowflake diagrams alongside the half-ladders we have used in our above 4-point example. The 6-point half-ladder and snowflake diagrams are shown in figures 8 and 9.

Rather than the single contact and 10 inequivalent exchange diagrams we now have $(2n-5)!! = 105$ diagrams [2] to work with in total, which are divided over $6!/2^3 = 90$ half ladder and $6!/(2^3\cdot 3!) = 15$ snowflake diagrams. The $\frac{1}{2^3}$ factors come from antisymmetry in all legs, and the $\frac{1}{3!}$ factor comes from the equivalence of the three prongs of the snowflake diagrams.

These numbers don't just come falling out of the sky of course, as they are tied to the diagrams themselves, and are the result of the permutations that leave the diagrams equivalent. The half-ladder diagrams, for instance, will remain entirely unchanged under the interchanging of the two legs that go into the first vertex, or those that come out of the last one, $\phi_a \leftrightarrow \phi_b$ and $\phi_e \leftrightarrow \phi_f$ in Figure 8. The same diagram is also unchanged under

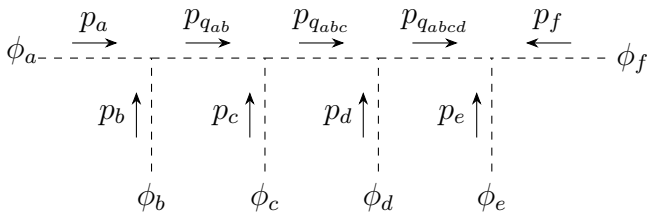

Figure 8: 6-point half-ladder BCJ diagram

the complete reversal of all the legs, meaning $\phi_a \leftrightarrow \phi_f$, $\phi_b \leftrightarrow \phi_e$, and $\phi_c \leftrightarrow \phi_d$ at the same time. This leads to the $\frac{1}{2^3}$ factor for the half-ladder diagrams.

The snowflake topology is significantly different than that of the half-ladder, and as it is far more constrained it will have less inequivalent options available. Exchanging any pair of external legs linking together will naturally leave the diagram invariant. Figure 9 shows how exchanging $\phi_a \leftrightarrow \phi_b$, $\phi_c \leftrightarrow \phi_d$, or $\phi_e \leftrightarrow \phi_f$ would not change anything about the forces at play in this interaction. These three equivalences once again give us a factor $\frac{1}{2^3}$, but the legs coming out of the central vertex can be connected to any of the external pairs in any order without changing the physics of these diagrams either. This leads to an additional factor of $\frac{1}{3!}$, for the $3 \times 2 \times 1$ ways one can pick the connections from each of the pairs of external legs to the central vertex. After one pair has been given a point to latch on to, one less point will be left over. All in all this means we are left over with 90 half-ladder and 15 snowflake diagrams.

These diagrams, by their topology, also show us that the momentum conservation rules will change somewhat, or at least, the way they are established will. The on-shell condition of p_6 remains as-is, but now we can form the equivalences of:

$$s_{1,2} = s_{3,4,5,6} = s_{3,4} + s_{3,5} + s_{3,6} + s_{4,5} + s_{4,6} + s_{5,6}, \tag{40}$$

and all its permutations. These follow from the fact that the half-ladder diagrams have all the momenta in a row, and thus taking the initial two going into the leftmost vertex should be the same as all 4 cascading together from the right side.

As long as we pick the same variables to solve for this set of equations will give us the same overall dependence as we saw before, and moreover will already contain the on-shell p_6^2 conservation law's additional constraint.

4.5.2 6-point Propagators, Numerators, and Amplitudes

A big difference between the 6-point and any of our previous examples is the fact that we now have to consider a lot more propagator terms than we had to before. Both types of diagrams will have three each. Those of the half-ladder diagrams will increase in scope with each vertex, while those of the snowflake diagrams will remain a bit more simple. As the half-ladder diagram passes the momentum on through each vertex an incoming leg contributes another instance of momentum to it. This means our full propagator term will

be a product of the three Mandelstam variables, like so:

$$D_1 = \frac{1}{s_{a,b}} \tag{41}$$

$$D_2 = \frac{1}{s_{a,b,c}} \tag{42}$$

$$D_3 = \frac{1}{s_{a,b,c,d}} = \frac{1}{s_{e,f}} \tag{43}$$

Where the last one can be taken as its equivalent counterpart. Constructing the propagator for these diagrams will then give us:

$$D_{\text{half-ladder}} = \frac{1}{s_{a,b}s_{a,b,c}s_{e,f}}. \tag{44}$$

The propagator terms for the snowflake diagram will be a tad simpler to compose, but there is still a product of three of them, as we have three internal lines leading into the snowflake's heart, as can be seen in Figure 9.

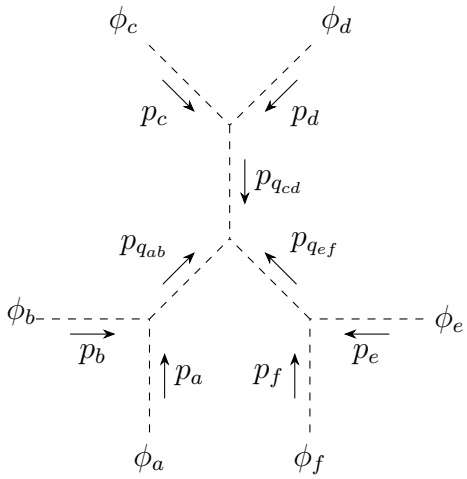

Figure 9: Snowflake diagram

One can then construct the overall propagator as follows:

$$D_{snowflake} = \frac{1}{s_{a,b}s_{c,d}s_{e,f}} \tag{45}$$

With these known the numerator terms can now be constructed. As above we will simply use the terms found in the work that lays the foundation for ours [2]. What is notable here however, is that the numerator factors for the snowflake diagrams were found to have another level of structure to them. Both the kinematic and flavour factors for the snowflake diagrams will have the form of [2]:

$$N^{\text{snowflake}}_{a,b,c,d,e,f} = N^{\text{half-ladder}}_{a,b,c,d,e,f} - N^{\text{half-ladder}}_{a,b,d,c,e,f}, \tag{46}$$

$$F^{\text{snowflake}}_{a,b,c,d,e,f} = F^{\text{half-ladder}}_{a,b,c,d,e,f} - F^{\text{half-ladder}}_{a,b,d,c,e,f}. \tag{47}$$

We can now present the formulas needed to find the full contributions to the amplitude from both the half-ladder and snowflake diagrams:

$$\mathcal{A}_{\text{half-ladder}} = \sum^{\text{diagrams}} \frac{N_{a,b,c,d,e,f} F_{a,b,c,d,e,f}}{s_{a,b} s_{a,b,c} s_{e,f}} \tag{48}$$

$$\mathcal{A}_{\text{snowflake}} = \sum^{\text{diagrams}} \frac{(N_{a,b,c,d,e,f} - N_{a,b,d,c,e,f})(F_{a,b,c,d,e,f} - F_{a,b,d,c,e,f})}{s_{a,b} s_{c,d} s_{e,f}}. \tag{49}$$

Both the kinematic and flavour numerators can be found, once again, by taking all of the possible combinations of Mandelstam variables (and flavour terms, for the flavour factor) and weighing them in a sum, which will then be subjected to Jacobi identities and demanded to factorise properly. However, in [2] a simplified version of the kinematic numerator was presented, which used only a subset of all the terms present in the 'full' kinematic numerator. That term is constructed from the identities below:

$$N_{a,b,c,d,e,f} = s_{a,b} P_{a,b,c,d,e,f} + \text{order reversed} \tag{50}$$

where $P_{a,b,c,d,e,f}$ is a physical parameter that is given by the expression:

$$\begin{aligned} P_{a,b,c,d,e,f} = -s_{e,f} \big(& s_{b,c} \left(-4 s_{a,f} + 4 \left(s_{b,d} + s_{c,d} + s_{c,e}\right) + 5 s_{d,e}\right) \\ & + s_{a,c} \left(-4 s_{a,f} + 4 \left(s_{b,d} + s_{c,d}\right) + s_{b,c} + 9 s_{d,e}\right) + 4 s_{a,b}^2 + 5 s_{a,c} s_{a,d} + s_{a,c}^2 \big) \\ & + 4 \left(s_{a,b} + s_{a,c} + s_{b,c}\right) \left(\left(s_{a,c} + s_{b,c}\right) \left(-s_{a,f} + s_{b,c} + s_{b,d} + s_{c,d}\right) + s_{b,c} s_{c,e}\right) \\ & - 4 s_{d,e} \left(s_{a,d} s_{b,c} + s_{a,c} \left(s_{b,d} + s_{c,d}\right)\right) + s_{e,f}^2 \left(4 s_{a,b} + 5 s_{a,c}\right), \end{aligned} \tag{51}$$

which is accompanied by a gauge transformation. This kinematic numerator, $N_{i,j,k,l,m,n}$ is composed of two overall terms, the latter the reverse order form of the first. When the full term is expanded all its subsequent terms are of order $s_{[2]}^4$, where $[n]$ gives the "order" of the Mandelstam variable, or in other words, how many of the momenta it draws together. As an example, $s_{a,b} \equiv s_{[2]}$, and $s_{a,b,c} = s_{a,b} + s_{a,c} + s_{b,c} \equiv s_{[3]}$.

We would like to note that this alternative compact numerator does not contain a set of gauge variables, whereas the full version of the kinematic numerator does, exactly like the flavour numerator, which we will present now.

The flavour numerator can, as a consequence of the overall process for finding these numerators that has already been discussed, be constructed from sets of:

$$\begin{aligned} F_{a,b,c,d,e,f} = s_{a,b}^2 \big(& 28 \delta_{a,f} \delta_{b,e} \delta_{c,d} - 28 \delta_{a,e} \delta_{b,f} \delta_{c,d} + 11 \delta_{a,b} \delta_{c,d} \delta_{e,f} + 13 \delta_{a,f} \delta_{b,d} \delta_{c,e} \\ & - 13 \delta_{a,d} \delta_{b,f} \delta_{c,e} - 34 \delta_{a,e} \delta_{b,d} \delta_{c,f} - 5 \delta_{a,d} \delta_{b,e} \delta_{c,f} + 25 \delta_{a,f} \delta_{b,c} \delta_{d,e} \\ & - 26 \delta_{a,c} \delta_{b,f} \delta_{d,e} + 8 \delta_{a,b} \delta_{c,f} \delta_{d,e} - 7 \delta_{a,e} \delta_{b,c} \delta_{d,f} + 26 \delta_{a,c} \delta_{b,e} \delta_{d,f} + 13 \delta_{a,b} \delta_{c,e} \delta_{d,f} \\ & - 9 \delta_{a,d} \delta_{b,c} \delta_{e,f} + 7 \delta_{a,c} \delta_{b,d} \delta_{e,f} \big) + \text{all Mandelstam combinations}, \end{aligned} \tag{52}$$

for all the different $s_{[2]}^2$ Mandelstam variable combinations. This factor has not been given in its full form. These numerator terms, as mentioned by those who found them originally [2], are "rather complicated" expressions. We will expand upon this by pointing out that showing them would take up a multitude of pages each.

The flavour numerator is also where we encounter gauge parameters, as they are a result of the varied possibilities in which the flavour numerator can satisfy its Jacobi relations. We have encountered these gauge parameters in the 4-point example already, where there

were only 3 in total. These were quite easily set to take on the values needed to turn the DC amplitude into one that mimics the Feynman amplitude. In this case however we have to work with 6 of them. We will however, be able to simplify our result to once again be gauge invariant, albeit in a somewhat reduced form due to computing power restraints.

With this we have hopefully sufficiently shown how one can construct an amplitude through the Double Copy method, and with that will be turning to the final point of interest for this work: the soft limit.

5 The Soft Limit

When examining an amplitude it can often be useful to take specific limits of energies or momenta. These can vary from overall low- or high-energy limits (InfraRed or UltraViolet limits), to even taking one of the specific particles' momenta to be zero. This is what we call the "soft limit".

We can of course not just take a particle's momentum to zero in and of itself, as it would cause problems in the mathematical representation of a theory, thus what we are really doing is a transformation of one, or in certain cases even multiple, of the external legs' the momenta of an interaction as follows:

$$p_a \to \varepsilon p_a. \tag{53}$$

Where we then take $\varepsilon \to 0$ to suppress the chosen leg's momentum and thus make it 'soft'.

The Soft Limit is an interesting extreme to take in a kinematic process due to the fact that a particle is taken to contribute (almost) no momentum to the interaction. A way of envisioning this is of course to consider a stationary target being hit by an accelerator beam, as practical experiments have done to probe the nature of particles and fields may times before. In this case however we are using a scalar field with no mass. This last aspect leads to the particle we enact this soft limit on to to not only contribute no momentum to the interaction, but to contribute (almost) no energy whatsoever, as it lacks even its rest mass. One could then imagine a soft limit of this kind to be akin to forcing an n-point interaction down to an (n-1)-point interaction. Given the nature of DBI's exclusively even interaction vertices this could make for some interesting considerations. It should thus hopefully be clear that the soft limit is a powerful tool with which one can probe the properties of a theory, or even groups of them, as, once again, the triplet of EFTs we have been hearing so much about share a bunch of properties in this regard.

The result of taking a soft limit depends of course on the nature of the theory. It has been found in [5] that the resulting soft behaviour of scalar Effective Field Theories (EFTs) like (Multi) DBI, NLSM, and SG depends on the ratio between the amount of fields and the amount of derivatives present in the interaction terms. The three scalar theories mentioned above behave in such a way under the soft limit that they form a special group within the category of EFTs, denoted as 'exceptional theories'. This means that their 'soft degree'–the ratio with which their amplitudes go to zero in the soft limit [4, 5]–is higher than one would naively expect from a look at the theory's Lagrangian. The authors conclude that these theories behave this way due to being the "natural EFT analogues of gauge theory and gravity" because they are single-parameter theories "with interactions strictly dictated by properties of the S-matrix." This same group of enhanced EFTs, and

their symmetries, can even be derived by imposing soft behaviour on the S-matrix, where the subset of exceptional EFTs is also already distinguishable. Clifford Cheung et al call this the "Soft Bootstrap" [3, 4, 5, 9].

5.1 Adler's Zero, Nambu-Goldstone Bosons, and Momentum Scaling

The amplitude after application of this soft limit will go to zero. This is a property found by Stephen L. Adler [10] and holds in general for theories with at least one Nambu-Goldstone boson (NGB) taken to its soft limit. This is a result of symmetry breaking within the EFT [4]. When one takes a theory that abides by a simple shift symmetry like:

$$\phi(x) \to \phi(x) + a \tag{54}$$

and introduces a degenerate ground state to that system, one once again–like we mentioned when discussing DBI–will find a spontaneously broken symmetry. What happens here is that the ground state has a continuous band of ground state "options" for the theory to occupy, granting it the freedom to spontaneously "pick" one, breaking the symmetry. The field degrees of freedom that arise from this process will have an accompanying Noether current, as they must, which will depend on the shift symmetry shown above. The scattering amplitude of a soft NGB found through this process is, in turn, closely related to the matrix element of the corresponding Noether current, J^μ [4]. The result of this is that the behaviour of an NGB in its soft limit is directly influenced by the internal shift symmetry that causes it to be.

The simple shift symmetry above is also what causes the soft limit of the amplitude of such a theory to behave as the Adler Zero [10, 4, 5] and if it is unaltered it will go to zero in the soft limit like $\mathcal{O}(\varepsilon)$. There is, however, a caveat here, as theories can have a different 'soft degrees', a term we mentioned before. The soft degree of a theory is the rate at which it goes to zero in the soft limit. This rate is defined by the power of ε with which the soft amplitude scales: $\mathcal{O}(\varepsilon^\sigma)$. The soft degree of our simple shift theory is thus $\sigma = 1$.

Different theories are often set apart by the exact scaling of this process, as it turns out to be a characteristic quality of the soft limit application to specific fields. The main factor that governs this behaviour is the amount of derivatives per field in the Lagrangian terms, as alluded to above and explained in [5] and [9], as it is intricately tied to the internal symmetries the theory respects.

5.2 Enhanced Soft Limits

We remember from the DBI chapter that its internal shift symmetry is given by equation (11):

$$\delta_{DBI}\phi(x) = c + b^\mu(x_\mu + \phi\partial_\mu\phi).$$

This is a bit of an expansion from our simple first order shift symmetry. An enhanced form, if you will. We can recognise our simple shift symmetry in this, but also find two more, more complex, terms. As such it will lead to a Noether current with a more defined behaviour, granting us further information on the soft limit properties of the theory beyond just the leading Adler Zero [4].

Something that sets DBI, and the other exceptional EFTs apart is the fact that their soft limit scales on a higher order than one would 'naively' expect from this ratio between

their fields and derivatives. To be precise, when taking the soft limit of $p_1 \to \varepsilon p_1$ one finds that instead of the expected $\sigma = 1$ soft degree implied by DBI's derivative to field ratio, we see the theory scale with $\mathcal{O}(\varepsilon^2)$, thus having a soft degree $\sigma = 2$. This is only possible because an internal cancellation takes place, cancellation of course alluding to destructive interference between different contributions of the amplitude. This is exactly why this has been dubbed an 'enhanced soft limit' [4].

Not surprisingly, the fact that DBI has an enhanced soft limit is the result of its shift symmetry being an enhanced form of the NGB-yielding-broken-shift-symmetry presented above. Specifically for DBI, the $b^\mu x_\mu$ term in the symmetry is what adds the enhanced degree. The field part of the symmetry is not of relevance here. In general it can even be shown that the shift symmetry's space-time degree is what defines the soft degree, thus our symmetry reaching up to $\mathcal{O}(x^n)$ causes the soft degree to reach the value of $n + 1$, indeed granting DBI a soft degree of $\sigma = 2$.

The choice of the 6-point interaction and the alternate approach through the DC should now of course be quite apparent. For any lower order interaction the only diagrams that can be constructed for this theory are half-ladders for the DC, and contact diagrams for Feynman. Snowflake and exchange diagrams only start appearing once we have 6 external legs to work with. The soft limit becomes interesting due to the fact that both the contact and exchange diagrams scale like $\mathcal{O}(\varepsilon)$ individually, but cancel out each other's $\mathcal{O}(\varepsilon)$ contributions when combined, leaving the full amplitude with a soft degree of $\sigma = 2$. This behaviour is rather unique, and as such it draws our attention. We will be trying to find out if this same behaviour is evident in the DC version to this amplitude, where one might then expect the contributions of the snowflake diagrams and half-ladder diagrams to scale like $\mathcal{O}(\varepsilon)$ individually as well, but to then cancel out and scale as $\mathcal{O}(\varepsilon^2)$ when taken together, as the overall amplitude must behave in the same way found through Feynman of course. Will the momentum scaling be manifest in the separate diagrams already, or will these contributions share their Feynman counterparts' soft limit interference behaviour?

6 Some Examples of Relevance

Before we continue on to the results we would like to present some examples of how the theory presented above is relevant to modern physics. We hope doing so can add some flavour to this work, and will show connections that theories like DBI and methods like the Soft Limit have to the field at large. The examples listed here are by no means exhaustive, and have been picked simply because they are interesting or noteworthy to us.

6.1 Weinberg's Soft Theorems

A noteworthy example of the soft limit and its effect on an interaction can be seen in Weinberg's soft theorems. Stephen Weinberg found that, when taking an interaction of *any* set of incoming particles, α, leading to *any* set of outgoing particles, β, and attaching a very low-energy (soft) photon or graviton to any of the legs of said interaction, the resulting amplitude will be highly constrained.

For both the photon and graviton the S-matrix element that would end up describing the soft-infused interaction ends up being defined simply by the S-matrix element that describes the initial, hard, interaction, multiplied simply by a single extra factor which is

completely independent of the hard interaction. These factors were aptly named Weinberg's Universal Soft Factors [11, 9]. Remarkably, these factors show that interactions infused with soft photons and gravitons will show universal factorisation behaviour, where the amplitudes behave according to a leading soft pole [11].

The addition of these soft particles also leads to infrared divergences, however one can show that, when considering both virtual and real soft infusions in the interaction, these divergences end up cancelling out. Another aspect resulting from Weinberg's calculations was the fact that neither the soft graviton nor soft photon would recognise spin of any of the other particles, along with a bunch of other quantum numbers, even though both particles, without their soft behaviour, were initially set up to couple only to interactions with zero total spin. The conclusion in the case of the soft graviton is that the coupling strength of gravity is *universal*, recovering General Relativity's famous equivalence principle quite simply through a rather general soft limit example [9].

Similar behaviour was found to apply to soft gluons, and more recently there has been much work done finding the subleading terms appearing in these soft theorems [12, 13].

6.2 The Classical Double Copy

The Double Copy itself was found as a connection between two specific theories, and was then enthusiastically used as a shortcut to gravity amplitudes, but it should of course already be very clear that this phenomenon is far more than a computational shortcut. The web that the DC ties together is vast and ever-growing.

Along with connecting field theories together through their shared respect of Jacobi relations it was recently found that the Double Copy is also capable of connecting them together through their equations of motion. Classical solutions of general relativity and YM were bound together through the "Kerr-Schild Double Copy" by finding a class of gauge-theory solutions [14] that connects to gravity through the Double Copy while also involving stationary Kerr-Schild metrics. The result was–among other things–the uncovering of the Schwarzschild and Kerr black holes as special cases in the reconstruction. Even further extensions of this approach can be found in [15], [16] and [17], and a short overview is given in [7].

6.3 Pions as NGBs and NLSM

As we are presenting DBI to probe the Double Copy through its enhanced soft limit we should also mention DBI's big brother, the Non-Linear Sigma Model. This theory is very relevant to NGBs and specifically their history, as it is intricately tied to Pions.

One of the first real-life NGBs relevant to field theory was the Pion. These quark-anti-quark pair mesons were discovered in cosmic rays by C. Powell and G. Occhialini in 1947 [18, 19] and have been the subject of many scattering experiments since, as their exchange allows for nucleons to change type. Initially however, they were conjectured by Hideki Yukawa, who proposed a new theory for strong and weak interactions in 1935 [20], where pions would be the strong force carriers, arising from the spontaneous breaking of the chiral symmetry that represents strong interactions. This theory did not account for their quark-anti-quark structure of course, and would end up being replaced by Quantum Chromodynamics later on, but it establishes the pion's importance even in the earlier days of field theory.

Since Yukawa's description our understanding of pions has developed further. We now know that they are the NGBs that arise from the spontaneous breaking of the axial-vector symmetries of the strong interaction Lagrangian [18], and they can be described using the NLSM, although only in the low-energy limit, as the NLSM describes massless NGBs, while pions have been found to be massive. This discrepancy is, however, not as much of a deal-breaker as one would expect, as the mass of pions consisting out of up, down, and strange quarks is sufficiently low to allow for NLSM to accurately describe their behaviour. This massive aspect is also why we have given pions the title of '*pseudo*-NGBs'. It was Yoichiro Nambu who had the insight to make this connection, and who showed that pions are indeed exactly NGBs when we approximate the lightest quark masses to zero.

NLSM is part of the trio of enhanced EFTs, together with DBI and SG. This means that NLSM will exhibit an enhanced soft limit as well. NLSM's Lagrangian can be given by [7]:

$$\mathcal{L}_{NLSM} = -\frac{1}{2}\partial_\mu\phi_a\partial^\mu\phi^a + \frac{\lambda^2}{6}f_{abe}f^{cde}\phi^a\partial_\mu\phi^b\phi_c\partial^\mu\phi_d + ... \tag{55}$$

We can see here that the fields, on average, have less than one derivative each, which means that the naive interpretation of the expected soft limit here [4] would be $\sigma = 0$. When we look at the internal shift symmetry of NLSM,

$$\delta\phi = c + \mathcal{O}(\phi^2), \tag{56}$$

which has no dependence on x but does contain a simple scalar shift symmetry–like the one we presented when discussing soft limits–we find this theory to have a soft degree of $\sigma = 1$, which is indeed one step higher than our naive expectation.

This (enhanced) soft behaviour will of course carry over to the lightest pions, as NLSM is still an excellent theory to describe these. As such there is indeed a soft pion theorem, similar to the Soft Weinberg theorems shown above, which dictates that the matrix element of an interaction that is infused with a soft pion can be found by taking the matrix element of the original interaction and multiplying it with a relatively simple factor [21]. In contrast to soft photon and gravitons however [11], the soft pion theorem does not exhibit an infrared divergence [21]. Surprisingly even, cosmological analogues of the soft pion theorem have been constructed, where the pion's nonlinear and shift symmetric properties were tied to curvature perturbations and velocities, which also shift in a similar manner [22, 23].

In the shadow of NLSM's pionic prestige DBI does not seem to have such a direct real-world comparison, but that shouldn't stop us from trying to use it in this research, as, along with NLSM and SG, it is an excellent theory with many interesting qualities.

Part II: Results and Discussion

7 Computational Methodology

Going from the theory presented above to calculated amplitudes is no small feat. The calculations needed for something as complex as Multi-DBI's 6-point interaction demand computational power far greater than is possible by hand and with limited time. For this exact reason the results presented in this section have been found through the use of Mathematica, with various packages used to make computation easier and more manageable. We will present a short overview of the work-flow of the programs used before then presenting the results found. Programs used will be provided alongside this document as attachments.

7.1 Feynman

The Feynman computation program we wrote depends on two main functions, namely, one for the contact and one for the exchange contribution. Both of these use xAct [24] to create full terms for each relevant diagram and their permutations, working with momentum 4-vectors. These contributions are then exchanged for Mandelstam variables to make handling the Soft Limit of the amplitude a lot easier to oversee. The 'backend' still using momentum variables was a choice made due to ease of parsing and exchanging exchange momenta labels for their constituent sum-of-external-legs equivalent. This last point was of course not needed for the contact diagram, but the similar architecture could be re-purposed for this diagram's permutations without much complications.

7.2 Double Copy

The Double Copy approach does not use momentum variables at all as the method works with Mandelstam variables directly. As such the xAct package was not needed for this computation. A challenge for this calculation is however that the rather large numerator terms make the computation of the Double Copy amplitude quite heavy. This led to unsolved problems attempting to remove terms that factorise incorrectly, as we will present in the coming chapters.

8 Soft Limit of the 6-point Feynman Amplitude

In this section we will present the calculated Feynman amplitude and its behaviour under the Soft Limit.

8.1 The 6-point Feynman Amplitude

The full Feynman amplitude of Multi-DBI was computed through Mathematica as explained above. As it is quite the gargantuan result we will focus on a single 'flavour channel.' That is to say, rather than presenting the complete amplitude we will only present the part of it that has flavour terms $t_{1,2}t_{3,4}t_{5,6}$. As all the flavour channels are identical to each other given permutations of indices this is of course just fine to do. Behaviour found

for this channel will thus be the same for all other channels. As such we present to you the full amplitude of this colour channel:

$$\begin{aligned}\mathcal{A}^{Full}_{12,34,56} = -2\,&(s_{1,4}s_{2,6}s_{3,5} - s_{1,2}s_{4,6}s_{3,5} + s_{1,4}s_{2,5}s_{3,6} + s_{1,3}s_{2,6}s_{4,5} - s_{1,2}s_{3,6}s_{4,5} \\ &+ s_{1,6}\left(-s_{2,5}s_{3,4} + s_{2,4}s_{3,5} + s_{2,3}s_{4,5}\right) + s_{1,3}s_{2,5}s_{4,6} \\ &+ s_{1,5}\left(-s_{2,6}s_{3,4} + s_{2,4}s_{3,6} + s_{2,3}s_{4,6}\right) - s_{1,4}s_{2,3}s_{5,6} - s_{1,3}s_{2,4}s_{5,6} + s_{1,2}s_{3,4}s_{5,6}) \\ &+ \frac{1}{s_{1,5,6}}\left(s_{1,4}s_{1,5}s_{1,6}s_{2,3} + s_{1,5}s_{1,6}s_{4,5}s_{2,3} + s_{1,5}s_{1,6}s_{4,6}s_{2,3} + s_{1,3}s_{1,5}s_{1,6}s_{2,4}\right. \\ &\quad - s_{1,2}s_{1,5}s_{1,6}s_{3,4} - s_{1,5}s_{1,6}s_{2,5}s_{3,4} - s_{1,5}s_{1,6}s_{2,6}s_{3,4} + s_{1,5}s_{1,6}s_{2,4}s_{3,5} \\ &\quad \left. + s_{1,5}s_{1,6}s_{2,4}s_{3,6}\right) + \frac{1}{s_{1,2,3}}\left(s_{1,3}s_{2,3}\left(s_{1,6}s_{4,5} + s_{2,6}s_{4,5} + s_{3,6}s_{4,5} + s_{1,5}s_{4,6}\right.\right. \\ &\quad \left.\left. + s_{2,5}s_{4,6} + s_{3,5}s_{4,6} - s_{1,4}s_{5,6} - s_{2,4}s_{5,6} - s_{3,4}s_{5,6}\right)\right) \\ &+ \frac{1}{s_{1,2,4}}\left(s_{1,4}s_{2,4}\left(s_{1,6}s_{3,5} + s_{2,6}s_{3,5} + s_{4,6}s_{3,5} + s_{1,5}s_{3,6} + s_{2,5}s_{3,6} + s_{3,6}s_{4,5}\right.\right. \\ &\quad \left.\left. - s_{1,3}s_{5,6} - s_{2,3}s_{5,6} - s_{3,4}s_{5,6}\right)\right) + \frac{1}{s_{1,2,5}}\left(s_{1,5}s_{2,5}\left(-s_{1,6}s_{3,4} - s_{2,6}s_{3,4}\right.\right. \\ &\quad \left.\left. - s_{5,6}s_{3,4} + s_{1,4}s_{3,6} + s_{2,4}s_{3,6} + s_{3,6}s_{4,5} + s_{1,3}s_{4,6} + s_{2,3}s_{4,6} + s_{3,5}s_{4,6}\right)\right) \\ &+ \frac{1}{s_{1,2,6}}\left(s_{1,6}s_{2,6}\left(-s_{1,5}s_{3,4} - s_{2,5}s_{3,4} - s_{5,6}s_{3,4} + s_{1,4}s_{3,5} + s_{2,4}s_{3,5} + s_{1,3}s_{4,5}\right.\right. \\ &\quad \left.\left. + s_{2,3}s_{4,5} + s_{3,6}s_{4,5} + s_{3,5}s_{4,6}\right)\right) + \frac{1}{s_{1,3,4}}\left(s_{1,3}s_{1,4}\left(s_{1,6}s_{2,5} + s_{3,6}s_{2,5} + s_{4,6}s_{2,5}\right.\right. \\ &\quad \left.\left. + s_{1,5}s_{2,6} + s_{2,6}s_{3,5} + s_{2,6}s_{4,5} - s_{1,2}s_{5,6} - s_{2,3}s_{5,6} - s_{2,4}s_{5,6}\right)\right) \\ &+ \frac{1}{s_{2,3,4}}\left(s_{1,6}s_{2,3}s_{2,4}\left(s_{2,5} + s_{3,5} + s_{4,5}\right) + s_{1,5}s_{2,3}s_{2,4}\left(s_{2,6} + s_{3,6} + s_{4,6}\right)\right. \\ &\quad \left. - \left(s_{1,2} + s_{1,3} + s_{1,4}\right)s_{2,3}s_{2,4}s_{5,6}\right) + \frac{1}{s_{2,5,6}}\left(-\left(\left(s_{1,2} + s_{1,5} + s_{1,6}\right)s_{2,5}s_{2,6}s_{3,4}\right)\right. \\ &\quad \left. + s_{1,4}s_{2,5}s_{2,6}\left(s_{2,3} + s_{3,5} + s_{3,6}\right) + s_{1,3}s_{2,5}s_{2,6}\left(s_{2,4} + s_{4,5} + s_{4,6}\right)\right) \\ &+ \frac{1}{s_{3,4,5}}\left(s_{1,6}\left(s_{2,3} + s_{2,4} + s_{2,5}\right)s_{3,5}s_{4,5} + s_{1,3}s_{2,6}s_{3,5}s_{4,5} + s_{1,4}s_{2,6}s_{3,5}s_{4,5}\right. \\ &\quad \left. + s_{1,5}s_{2,6}s_{3,5}s_{4,5} - s_{1,2}s_{3,5}s_{3,6}s_{4,5} - s_{1,2}s_{3,5}s_{4,6}s_{4,5} - s_{1,2}s_{3,5}s_{5,6}s_{4,5}\right) \\ &+ \frac{1}{s_{3,4,6}}\left(s_{1,3}s_{2,5}s_{3,6}s_{4,6} + s_{1,4}s_{2,5}s_{3,6}s_{4,6} + s_{1,6}s_{2,5}s_{3,6}s_{4,6}\right. \\ &\quad + s_{1,5}\left(s_{2,3} + s_{2,4} + s_{2,6}\right)s_{3,6}s_{4,6} - s_{1,2}s_{3,5}s_{3,6}s_{4,6} - s_{1,2}s_{3,6}s_{4,5}s_{4,6} \\ &\quad \left. - s_{1,2}s_{3,6}s_{5,6}s_{4,6}\right) + \frac{1}{s_{3,5,6}}\left(s_{1,3}s_{2,4}s_{3,5}s_{3,6} + s_{1,5}s_{2,4}s_{3,5}s_{3,6} + s_{1,6}s_{2,4}s_{3,5}s_{3,6}\right. \\ &\quad + s_{1,4}\left(s_{2,3} + s_{2,5} + s_{2,6}\right)s_{3,5}s_{3,6} - s_{1,2}s_{3,4}s_{3,5}s_{3,6} - s_{1,2}s_{3,5}s_{4,5}s_{3,6} \\ &\quad \left. - s_{1,2}s_{3,5}s_{4,6}s_{3,6}\right) + \frac{1}{s_{4,5,6}}\left(s_{1,4}s_{2,3}s_{4,5}s_{4,6} + s_{1,5}s_{2,3}s_{4,5}s_{4,6} + s_{1,6}s_{2,3}s_{4,5}s_{4,6}\right. \\ &\quad + s_{1,3}s_{2,4}s_{4,5}s_{4,6} + s_{1,3}s_{2,5}s_{4,5}s_{4,6} + s_{1,3}s_{2,6}s_{4,5}s_{4,6} - s_{1,2}s_{3,4}s_{4,5}s_{4,6} \\ &\quad \left. - s_{1,2}s_{3,5}s_{4,5}s_{4,6} - s_{1,2}s_{3,6}s_{4,5}s_{4,6}\right)\end{aligned} \tag{57}$$

This is, quite frankly, a horrible mess to work with, and also lacks one very integral step: it still expressed all 15 possible Mandelstam variables relevant to a 6-point interaction. Now, rather than working directly with this, we will split the amplitude up into its constituent parts, namely the Contact and Exchange contributions, simplify those while expressing them in only 9 independent Mandelstam variables, and discuss only the parts of them that

will scale with $\mathcal{O}(\varepsilon)$ once the soft limit is applied, as those are the terms relevant to the Soft Limit's cancellation.

8.2 Soft Limit of the 6-point Feynman Amplitude

Thus, we present the contribution of the contact amplitude that scales with $\mathcal{O}(\varepsilon)$ after expressing it in Mandelstam variables $s_{1,2}, s_{1,3}, s_{1,4}, s_{1,5}, s_{2,3}, s_{2,4}, s_{3,4}, s_{3,5}, s_{4,5}$:

$$\begin{aligned}\mathcal{A}^{Contact}_{12,34,56} \sim & -2s_{1,5}s^2_{3,4} - 2s_{1,5}s_{2,3}s_{3,4} - 2s_{1,5}s_{2,4}s_{3,4} + 2s_{1,2}s_{3,5}s_{4,5} \\ & - 2s_{1,5}s_{3,5}s_{3,4} - 2s_{1,5}s_{4,5}s_{3,4} + 2s_{1,3}s_{3,5}s_{4,5} + 2s_{1,4}s_{3,5}s_{4,5} \\ & - 2s_{1,5}s_{2,3}s_{2,4} - 2s_{1,5}s_{2,4}s_{3,5} - 2s_{1,5}s_{2,3}s_{4,5} \\ & + 2s_{1,4}s_{3,5}s_{3,4} + 2s_{1,3}s_{4,5}s_{3,4} + 2s_{1,3}s_{2,4}s_{4,5} + 2s_{1,4}s^2_{3,5} - 4s_{1,4}s_{2,3}s_{3,5} + 2s_{1,3}s^2_{4,5}. \quad (58)\end{aligned}$$

Logically, no factorisation is found here.

The $\mathcal{O}(\varepsilon)$ contribution to this interaction provided by the exchange diagrams is as follows:

$$\begin{aligned}\mathcal{A}^{Exchange}_{12,34,56} \sim & -2s_{1,5}s^2_{3,4} - 2s_{1,5}s_{2,3}s_{3,4} - 2s_{1,5}s_{2,4}s_{3,4} + 2s_{1,2}s_{3,5}s_{4,5} \\ & - 2s_{1,5}s_{3,5}s_{3,4} - 2s_{1,5}s_{4,5}s_{3,4} + 2s_{1,3}s_{3,5}s_{4,5} + 2s_{1,4}s_{3,5}s_{4,5} \\ & - 2s_{1,5}s_{2,3}s_{2,4} - 2s_{1,5}s_{2,4}s_{3,5} - 2s_{1,5}s_{2,3}s_{4,5} \\ & + \frac{2s_{1,4}s_{2,4}s_{3,5}s_{3,4}}{s_{1,2,4}} + \frac{2s_{1,3}s_{2,3}s_{4,5}s_{3,4}}{s_{1,2,3}} + \frac{2s_{1,3}s_{2,3}s_{2,4}s_{4,5}}{s_{1,2,3}} \\ & + \frac{2s_{1,4}s_{2,4}s^2_{3,5}}{s_{1,2,4}} + \frac{2s_{1,4}s_{2,3}s_{2,4}s_{3,5}}{s_{1,2,4}} + \frac{2s_{1,3}s_{2,3}s^2_{4,5}}{s_{1,2,3}}, \quad (59)\end{aligned}$$

expressed in the same variables. Here of course we do see propagators pop up, as they are provided by the exchanged virtual particle. Terms that have no propagator here will have had them already divided out through application of momentum conservation rules and grouping numerators together to cancel out denominators. We would like to point out the fact that the propagator terms that have been divided out are specifically the ones that don't contain p_1.

Now as we add the two together we find a lot of terms will cancel out naturally, as the terms of the exchange contribution that lost their propagators are the exact opposite of terms in the contact's $\mathcal{O}(\varepsilon)$ contribution. The first 11 terms of both contributions shown above cancel out, which leaves us with the following:

$$\begin{aligned}\mathcal{A}^{Full}_{12,34,56}\mathcal{O}(\varepsilon) \sim & -2s_{1,3}s^2_{4,5} - 2s_{1,3}s_{2,4}s_{4,5} - 2s_{1,3}s_{3,4}s_{4,5} \\ & - 2s_{1,4}s^2_{3,5} - 2s_{1,4}s_{2,3}s_{3,5} - 2s_{1,4}s_{3,4}s_{3,5} \\ & + \frac{2s_{1,3}s_{2,3}s^2_{4,5}}{s_{1,2,3}} + \frac{2s_{1,3}s_{2,3}s_{2,4}s_{4,5}}{s_{1,2,3}} + \frac{2s_{1,3}s_{2,3}s_{3,4}s_{4,5}}{s_{1,2,3}} \\ & + \frac{2s_{1,4}s_{2,4}s^2_{3,5}}{s_{1,2,4}} + \frac{2s_{1,4}s_{2,3}s_{2,4}s_{3,5}}{s_{1,2,4}} + \frac{2s_{1,4}s_{2,4}s_{3,4}s_{3,5}}{s_{1,2,4}}. \quad (60)\end{aligned}$$

One can quickly see that taking the $p_1 \to \varepsilon p_1$ soft limit here will suppress all the $s_{1,i}$ terms in the propagators compared to the ones not containing p_1, as the 3-variable propagators have the form:

$$\frac{1}{s_{a,b,c}} = \frac{1}{s_{a,b} + s_{a,c} + s_{b,c}}$$

Which for $a = 1$ in our soft limit gives us reduced forms of these propagators:

$$\frac{1}{s_{1,b,c}} = \frac{1}{s_{1,b} + s_{1,c} + s_{b,c}} \sim \frac{1}{s_{b,c}}.$$

This leaves us only with propagators of $\frac{1}{s_{2,3}}$, $\frac{1}{s_{2,4}}$, and $\frac{1}{s_{3,4}}$, which then neatly cancel with equivalent terms above. After the soft limit gets rid of the remaining propagators in this order we can see that the terms from the contact and exchange contributions cancel out rather nicely.

$$\begin{aligned}\mathcal{A}^{SL}_{12,34,56}[\mathcal{O}(p_1)] \sim \\ &- 2s_{1,3}s_{4,5}^2 + 2s_{1,3}s_{4,5}^2 \\ &- 2s_{1,3}s_{2,4}s_{4,5} + 2s_{1,3}s_{2,4}s_{4,5} \\ &- 2s_{1,3}s_{3,4}s_{4,5} + 2s_{1,3}s_{3,4}s_{4,5} \\ &- 2s_{1,4}s_{3,5}^2 + 2s_{1,4}s_{3,5}^2 \\ &- 2s_{1,4}s_{2,3}s_{3,5} + 2s_{1,4}s_{2,3}s_{3,5} \\ &- 2s_{1,4}s_{3,4}s_{3,5} + 2s_{1,4}s_{3,4}s_{3,5} \\ &= 0 \quad (61)\end{aligned}$$

Thus it can be seen that all the $\mathcal{O}(\varepsilon)$ contributions to this amplitude vanish in the Soft Limit, leaving it to make its way to 0 along the square power of $varepsilon$, rather than the single one. This result is not shocking, as it was already known to be a defining feature of the theory, yet it might serve to illuminate the possibilities of the Double Copy contributions doing the same. The contributions cancel out mathematically due to the 'soft propagators' being able to align the $\mathcal{O}(\varepsilon)$ terms of both contributions to this amplitude, dividing out an extraneous Mandelstam variable.

It is worth a moment of consideration to note that the factorisation channels have most certainly *not* all disappeared. Rather, they seem to be ordered such that any channels that aren't reduced by the soft limit and don't divide out naturally, will only contribute to higher order ε scaling. We find that remaining propagators not containing p_1, like $\frac{1}{s_{3,4,5}}$ will be part of terms that scale only with ε^2 or higher.

The amplitude's factorisation terms sort themselves out nicely in groups of numerators which scale with ε^2 or above already, the factorisation of which is not an issue either way; and all the factorisation terms that *do* scale with ε, which will have a denominator that reduces to a single Mandelstam variable in the soft limit, allowing the term to lose its factorisation and interact with terms from the contact amplitude. The full ε amplitude of this channel is given in the 9 independent Mandelstam variables in the appendix for those curious enough to see for themselves.

9 Discussing the DC Amplitude

It is at this point that we must sadly present an amplitude that does not comply with what we expect the DBI amplitude to look like. The amplitude that was found through the double copy shows a large amount of 3-point factorisation, which is not allowed in DBI. This factorisation is expected to cancel out, like they did quite straight-forwardly in the 4-point case. Many attempts were made to simplify the result found, but none were successful, as incorrectly factorising terms remained.

9.1 Overall Amplitude

There were two options to find the amplitude, one through the full kinematic numerator, and the other through the compacted version presented in [2], both mentioned in the Double Copy chapter. The compacted amplitude was, logically, not as large as the full one, and lacked a second set of gauge variables that made the whole thing a lot more simple to work with. Sadly however, it does not seem to factorise the right way. This may be an error on our part in computation, or could be an error in notation in the cited source, but after countless tries to simplify the overall amplitude, and selecting specific points in momentum space to test the overall factorisation, we found 3-point vertices still accounted for.

Testing factorisation through selecting specific points in momentum space was done by replacing all-but-one of the 9 independent Mandelstam variables with a prime number–so as to avoid unwanted issues in the propagators–and picking any specific gauge at random. When multiplying the result by the specific Mandelstam variable that was kept unspecified and sending its value to 0 the result will be 0 if the amplitude does not contain factorisation channels of this variable. One can repeat this process for all Mandelstam variables. This worked because of the significant simplifications enacted on the amplitude, as it would not work on its full form. We found the results of these samples to turn up with nonzero values, thus we must conclude the factorisation did not work out.

Using the full kinematic numerator, including the extra set of gauge variables, leaves us with a sum of over 30 million terms. This can of course be simplified by grouping gauge variables together with sets of Mandelstam and flavour terms, and analysing the amplitude will of course only require a single flavour channel. Even with these simplifications this amplitude still remains sufficiently large that it is very hard to handle. It still reaches well beyond 8 million terms in this form. A wonderful upside of this ample amplitude, however, is that it *does* in fact factorise correctly when testing the factorisation in specific points in momentum space.

9.2 Factorisation

The overall factorisation of the compacted amplitude did not work out, and as such it is not an amplitude we can consider for this research. The full numerator factors, however, do make for an amplitude that factorises correctly, and thus may indeed be able to represent the same answer we found through Feynman. An interesting feat here is the difference between the way the contact and exchange diagrams behave in Feynman formalism, and the way the half-ladder and snowflake diagrams behave in the Double Copy. These latter two diagram types do not factorise the right way *independently*. This means that the incorrectly factorising terms arising from these diagrams only disappear by way of cancelling each other out. Moreover, when picking specific points in momentum space for our Mandelstam variables while keeping the contributions of both diagram types separate we find that that the resulting contributions containing invalid factorisation are exactly the opposite of one another, and will thus indeed cancel each other out exactly.

The fact that the full amplitude was found to factorise correctly when picking specific points in momentum space is good news, however it does not mean we managed to align this amplitude with the Feynman result, as the amplitude we were working with was, as mentioned, far too large to properly handle (by us, anyways). As such, when the Mandelstam variables were left as variables we were not able to simplify the amplitude, or even get rid of all the incorrectly factorising terms. We suspect that a lot of processing

power and time will be needed to properly manipulate this amplitude to untangle all of the terms in the exact way that manages to cancel out all of the unwanted factorisation.

Even a single flavour channel of the amplitude will contain many terms of the form:

$$-\frac{5x_6z_6s_{4,5}^6}{42s_{3,4}\left(s_{3,4}+s_{3,5}+s_{4,5}\right)\left(s_{1,3}+s_{1,4}+s_{1,5}+s_{3,4}+s_{3,5}+s_{4,5}\right)}. \tag{62}$$

Here we have an $s_{[2]}^6$ divided by 3 propagator terms. One simple Mandelstam variable, one 4-point factorisation term: $s_{3,4,5}$, and a more complicated factorisation term, that, upon reversing the momentum conservation rules we applied, can be shown to represent $s_{2,6}$. A contribution like this could, when accompanied by a complementary set of similar contributions that multiply with $s_{4,5}^5$ and together form the sum

$$x_6z_6\left(s_{1,3}+s_{1,4}+s_{1,5}+s_{3,4}+s_{3,5}+s_{4,5}\right)s_{4,5}^5, \tag{63}$$

or

$$x_6z_6\left(s_{3,4}+s_{3,5}+s_{4,5}\right)s_{4,5}^5, \tag{64}$$

cancel out either of these summed propagator terms. The former being the case would get rid of one of the unwanted factorisation terms, but would still leave us with $s_{3,4}$, while the latter being cancelled out would not necessarily help us in getting rid of the invalid factorisation directly, but might allow this term, which–by nature of containing a 4-point factorisation denominator–originates from a half-ladder diagram, to cancel out against a term hailing from a snowflake diagram.

Since we know that the amplitude *does* factorise correctly in specific points in momentum space we must conclude that it is indeed capable of simplifying into a correct form of the DBI amplitude. The mechanisms of this process, as presented above, are cancellation within the term itself, by way of seeing unwanted propagator terms divide out, and cancellation between the different types of diagrams. We will present the forms that terms in this amplitude can take below:

$$s_{[2]}^3 \sim s_{a,b}s_{c,d}s_{e,f} \tag{65}$$

$$\frac{s_{[2]}^4}{s_{[3]}} \sim \frac{s_{a,b}s_{c,d}^3}{s_{c,d,e}} \tag{66}$$

$$\frac{s_{[2]}^4}{s_{[2]}} \sim \frac{s_{a,b}^4}{s_{a,c}} \tag{67}$$

$$\frac{s_{[2]}^5}{s_{[2]}^2} \sim \frac{s_{a,c}s_{a,e}s_{b,d}^2s_{c,e}}{s_{a,b}s_{c,d}} \tag{68}$$

$$\frac{s_{[2]}^5}{s_{[2]}s_{[3]}} \sim \frac{s_{d,e}^5}{s_{c,d,e}s_{b,f}} \tag{69}$$

$$\frac{s_{[2]}^5}{s_{[3]}s_{[4]}} = \frac{s_{[2]}^5}{s_{[2]}s_{[3]}} \tag{70}$$

$$\frac{s_{[2]}^6}{s_{[2]}s_{[3]}s_{[4]}} = \frac{s_{[2]}^6}{s_{[2]}s_{[3]}s_{[2]}} \tag{71}$$

Where we have picked terms from the amplitude at random simply to illustrate their form. $s_{[n]}$ gives amount of combined momenta in the Mandelstam variable. $s_{[2]}$ and $s_{[4]}$ terms

are effectively the same due to momentum conservation laws, but depending on which basis one picks to represent the amplitude one or the other will emerge. For instance $s_{2,5}$ can be written out as the negative sum of all the other independent Mandelstam variables through the on-shell p_6^2 constraint, as we have discussed above. The terms we do not mind seeing in this amplitude are of course the quartic propagators: $s_{[3]}$, but those are far from the only denominators we find in this amplitude. All terms above will be accompanied by two gauge variables, z_i and x_j, coming from the kinematic and flavour numerators respectively. These have been left out for simplicity.

9.3 Gauge Dependence

Upon further inspection we managed to find that the overall amplitude can be, when once again severely reduced, written out as a sum of Mandelstam term products multiplied by a sum of kinematic gauge variables, and then multiplied by a set of flavour gauge variables. This shows us that the full amplitude is indeed gauge invariant, as it o course should be. We also found that the independent diagram types, however, do not combine into such a tidy result, even upon simplification, and are therefore not gauge invariant by themselves. This may fit the nature of individual diagrams though, as these do not have to be gauge-invariant, since they are not observable by themselves. Only the overall amplitude is observable.

9.4 Reconciling the Double Copy and Feynman Approach

We have found that the Double Copy amplitude will indeed factorise correctly upon cancellation from both different types of diagrams. Before we can completely reconcile both of these amplitudes, however, we must still select a gauge for the DC amplitude. Our Feynman method does not result in an amplitude that has any gauge-dependence, so neither should this one. Selecting a gauge, or finding a range of gauges that give us the same answer, like picking $z_{3,2} = z_{3,1}$ and $z_{1,2} = 1/(3z_{3,1})$ for the 4-point DC, amounts to constraining the kinematic and flavour numerators, as that is where these terms come from. This grants us some potential insight into the nature and application of the DC itself, as it indicates that the numerator terms can, and have to, be constrained further than just the Jacobi identities and correct factorisation demand.

To illustrate this we will draw attention to the fact that the DC diagrams contain two different sectors of contributions each, one that factorises "correctly" and fits the DBI amplitude, and another that*doesn't* factorise correctly, but vanishes. We will call these, respectively, the Singular, and Regular parts. The contents of the individual diagrams are heavily dependent on the choice of gauge, and it is possible that, when constrained in the right way, one might be able to recover only the Singular contributions directly.

Another feature that factors in to this is the fact that the factorisation of both approaches has facets of facsimile. The Feynman diagram types have contributions that contain either a 4-point propagator, or no propagators at all, contributed by, respectively, the exchange and contact diagram. In the DC case the amplitude we end up with will have to be the same as the Feynman case. Under the assumption that it is there will once again need to be 4-point factorising terms and terms without factorisation. Due to the way the diagrams are set up in the DC we can see that only the half-ladder diagrams are capable of contributing a 4-point factorisation denominator. The snowflake diagrams, on the other hand, will, once their factorisation is "resolved" contribute only terms without factorisation. There

seems to be a potential comparison one can draw between the types of diagrams. The question then becomes where the terms that disappear in the soft limit originate.

9.5 Soft Limit of the Double Copy

Looking back at equations 58, 59, and 60 we can see the terms that are relevant to the soft limit cancellation of the $\mathcal{O}(\varepsilon)$ part of the 6-point DBI amplitude. These contributions are not dependent on the Feynman method, as the DC and Feynman method (and any other we might be able to think of) will have to agree on the result of the amplitude. The amplitude is method independent after all. This means that, before we start applying the soft limit, we need to recover these exact same terms from our DC amplitude.

As discussed shortly above the relevant terms for the soft limit cancellation are those found in quation 58 and 59, shown here again for convenience:

$$\begin{aligned}\mathcal{A}^{Contact}_{12,34,56} \sim & -2s_{1,5}s^2_{3,4} - 2s_{1,5}s_{2,3}s_{3,4} - 2s_{1,5}s_{2,4}s_{3,4} + 2s_{1,2}s_{3,5}s_{4,5} \\ & - 2s_{1,5}s_{3,5}s_{3,4} - 2s_{1,5}s_{4,5}s_{3,4} + 2s_{1,3}s_{3,5}s_{4,5} + 2s_{1,4}s_{3,5}s_{4,5} \\ & - 2s_{1,5}s_{2,3}s_{2,4} - 2s_{1,5}s_{2,4}s_{3,5} - 2s_{1,5}s_{2,3}s_{4,5} \\ & + 2s_{1,4}s_{3,5}s_{3,4} + 2s_{1,3}s_{4,5}s_{3,4} + 2s_{1,3}s_{2,4}s_{4,5} + 2s_{1,4}s^2_{3,5} - 4s_{1,4}s_{2,3}s_{3,5} + 2s_{1,3}s^2_{4,5}\end{aligned} \tag{72}$$

$$\begin{aligned}\mathcal{A}^{Exchange}_{12,34,56} \sim & -2s_{1,5}s^2_{3,4} - 2s_{1,5}s_{2,3}s_{3,4} - 2s_{1,5}s_{2,4}s_{3,4} + 2s_{1,2}s_{3,5}s_{4,5} \\ & - 2s_{1,5}s_{3,5}s_{3,4} - 2s_{1,5}s_{4,5}s_{3,4} + 2s_{1,3}s_{3,5}s_{4,5} + 2s_{1,4}s_{3,5}s_{4,5} \\ & - 2s_{1,5}s_{2,3}s_{2,4} - 2s_{1,5}s_{2,4}s_{3,5} - 2s_{1,5}s_{2,3}s_{4,5} \\ & + \frac{2s_{1,4}s_{2,4}s_{3,5}s_{3,4}}{s_{1,2,4}} + \frac{2s_{1,3}s_{2,3}s_{4,5}s_{3,4}}{s_{1,2,3}} + \frac{2s_{1,3}s_{2,3}s_{2,4}s_{4,5}}{s_{1,2,3}} \\ & + \frac{2s_{1,4}s_{2,4}s^2_{3,5}}{s_{1,2,4}} + \frac{2s_{1,4}s_{2,3}s_{2,4}s_{3,5}}{s_{1,2,4}} + \frac{2s_{1,3}s_{2,3}s^2_{4,5}}{s_{1,2,3}}\end{aligned} \tag{73}$$

We know for a fact that the latter set of terms at one point all factorised with some Mandelstam variable $s_{[3]}$, although, rather conveniently, those parts that do not contain the soft momentum can already be divided out. Originally thus, all these terms contained some 4-point factorisation, and as such it is likely that they have analogous terms in the half-ladder contribution of the DC amplitude, since its propagator structure is defined by equation 48:

$$\frac{1}{s_{a,b}s_{a,b,c}s_{e,f}}. \tag{74}$$

The former set of terms (72) will of course *not* have factorisation, and will, in the case of the Feynman amplitude, have not had any to begin with. We do not know if this is the case for the DC amplitude since there are a few possibilities here.

The first option we can consider is that these terms will all have analogous terms coming from the DC's snowflake diagrams, as these diagrams have a propagator structure of (49):

$$\frac{1}{s_{a,b}s_{c,d}s_{e,f}}, \tag{75}$$

Which will have to be divided out for the terms to be valid in the amplitude. This is rather straight-forward and supports some conjecture we will expand upon further down.

The other option is that these terms will instead be contributed by the half-ladders after a lot of cancellation of factorisation has happened. Even though we do not know exactly what is going on here, we deem the thought that both sides of this cancellation originate from the half-ladder diagrams somewhat unlikely. One would think that the permutative structure of the numerators and all the inequivalent contributions in the diagrams would prevent equivalent terms from popping up in such a fashion, although there is room for different $s_{[2]}$ propagators dividing out to form the denominator-less half of this sum. We can only speculate on the nature of these contributions for now.

There is also a possibility that coincides with the last option presented, which is that the snowflake diagram contributes only factors that serve to cancel out the incorrect factorisation of the half-ladder diagrams, and is then wholly exhausted after doing so. We deem this particularly unlikely, as we were already able to find*some* terms originating from snowflake diagrams whose factorisation divided out wholly. If this were the case though the snowflake diagrams' contribution would be simply that of providing counterterms for the half-ladder diagrams. We restate that we do not consider this a probable option, but it must be stated as a possibility nevertheless.

Something we *do* know is that the amplitude does in fact contain terms that, initially, scale like $\mathcal{O}(\varepsilon)$ when the soft limit is applied. This is simply a consequence of the amplitude itself having to be recovered before applying the Soft Limit. When working out the math these terms will, of course, cancel out, but the manner in which they do is still uncertain, and reflects the ways in which the amplitude's terms are built up through the DC. The options would thus either be that we find the same pattern of inter-diagrammatic soft cancellation, or the diagrams already exhibit a manifest $\sigma = 2$ degree.

If there is no cancellation between diagrams, then the snowflake diagrams scale like $\mathcal{O}(\varepsilon^2)$ manifestly without much work needed to be done, but the half-ladder diagrams will then need the $\sigma = 1$ terms to be cancelled out by their own/each other's contributions. They will then exhibit a $\sigma = 2$ soft degree manifestly, but only after some mathematical shenanigans. The second option might also contain the possibility that the snowflakes only provide counterterms.

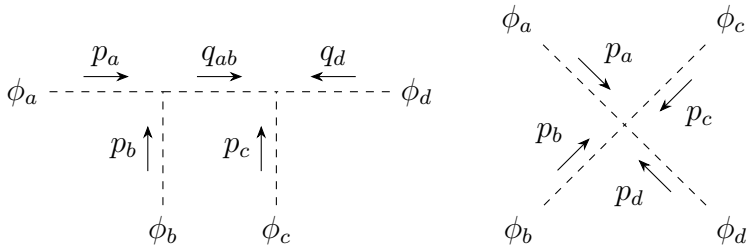

(a) 4-point Half-ladder (b) 4-point Contact

Figure 10: 4-point Half-ladder and Exchange

9.6 Potential Further Constraints and Links to Feynman

The Double Copy amplitude, as we have presented it, saw far more terms internally generated than are needed for the amplitude to be valid. We found that these excess (and invalid) terms cancel out between diagrams, and have found this phenomenon to be potential cause for some interesting speculation.

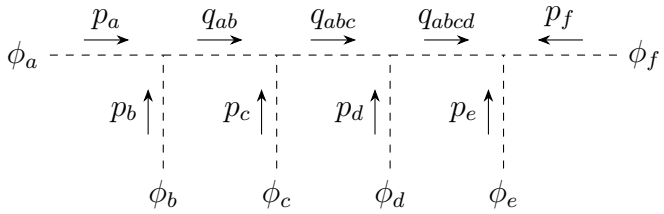

Figure 11: 6-point Half-ladder

In the event that the snowflake diagrams do indeed contribute a share that doesn't end up being spent entirely as counterterms we might conjecture that there is a potential overlap between the exchange and half-ladder diagrams, and then potentially even between the contact and snowflakes. The initial thought behind this is of course the fact that all the terms that (without simplifying the amplitude by dividing them out) factorise with quartic propagators must originate from the exchange and the half-ladder contributions respectively. We consider though, that there might be some topological connections between these two types of diagrams in particular as well.

We used the 4-point example of DBI to show the workings of both the Feynman method and the Double Copy, and in doing so showed that the contribution from the 4-point half-ladder is exactly identical to that of the 4-point contact diagram. This makes sense as there are no other diagrams to be composed for this interaction. This equivalence might then, however, be extended into the 6-point's half-ladder and exchange diagrams. The exchange diagram is composed of two 4-point contact diagrams connected by a propagator, while one can divide up the 6-point half-ladder into two 4-point half-ladder diagrams connected by a propagator all the same, as is shown in Figures 10, 11, and 12.

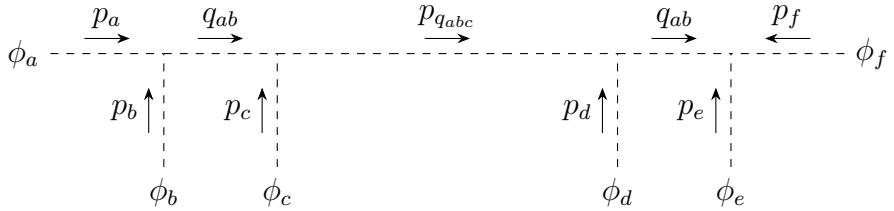

(a) 6-point Half-ladder reshape

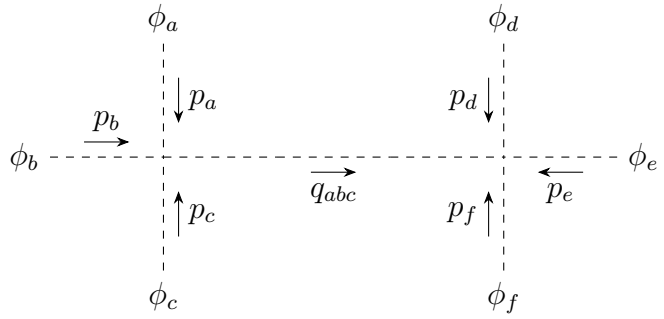

(b) 6-point Exchange reshape

Figure 12: Reshaped diagrams

A caveat we are compelled to add here is of course the fact that the DC diagram contributions are *not* gauge independent, so this phenomenon would only be possible for a specific gauge choice. Regardless of this though, one might ask the question: Are the

snowflake diagrams exactly equivalent to the contact diagram in their contributions? If the half-ladder and exchange diagrams are, and the regular part with invalid factorisation is no longer obstructing us through having picked a gauge that only causes the numerators to generate singular terms, then all that is left to contribute to the amplitude is the contact diagram's share. In the same topological reasoning as for the exchange and half-ladder diagram, the snowflakes do show all legs connecting (in this case through internal propagators) to a central vertex. This would thus lead us to present the possibility that these diagrams are indeed simply restructured forms of one another, mappings from one method to the other. This hypothesis, if true, has certain implications about the numerators, since we could now potentially reconstruct the 6-point half-ladder diagram from two 4-point half-ladders, giving us a potential new constraint on the 6-point numerator factors, or moreso a new way to construct them. We must stress, however, that there is no proof for this, and as such we are merely speculating about the possibilities.

We remember from the Double Copy 6-point half-ladder amplitude that:

$$\mathcal{A}_{\text{half-ladder}} = \sum^{\text{diagrams}} \frac{N_{a,b,c,d,e,f} F_{a,b,c,d,e,f}}{s_{a,b} s_{a,b,c} s_{e,f}} \tag{76}$$

Which we might possibly choose to rewrite, like such:

$$\mathcal{A}^{\text{singular}}_{\text{half-ladder}} = \sum^{\text{diagrams}} \frac{N_{a,b,c,q} F_{a,b,c,q}}{s_{a,b}} \frac{1}{s_{a,b,c}} \frac{N_{q,d,e,f} F_{q,d,e,f}}{s_{e,f}}. \tag{77}$$

Where we simply take the left and right half-ladder diagrams separately and connect them through the propagator that carries the momentum from one 'vertex' to the other.

This, in turn, would then lead us to suspect that the individual 6-point kinematic and flavour numerators can be constructed from compounded 4-point numerator terms:

$$N_{a,b,c,d,e,f} = N_{a,b,c,q} N_{q,d,e,f} \tag{78}$$

$$F_{a,b,c,d,e,f} = F_{a,b,c,q} F_{q,d,e,f}, \tag{79}$$

which might be of aid in constructing the fitting forms of the 6-point flavour numerator, and could simplify higher point Double Copy calculations. It might also come with the benefit of being able to find the amplitude without having to account for a large amount of terms with invalid factorisation, as numerators constructed in this way will not cause regular parts to appear in the first place.

Checking the numerators through this method should not be particularly hard, but upon a limited amount of testing this hypothesis we weren't able to find conclusive results, and as our time is finite we will pat ourselves on the back for trying and leave the rest up to someone else.

When applying the DC to higher point amplitudes and comparing the results to the lower point analogues it would seem strange that such a vast array of, for all intents and purposes, 'useless terms' shows up. It might thus be possible to construct this amplitude in such a way that they only generate viable terms, namely, those with correct factorisation. The connection one could make between the two 4-point half-ladders and the single 6-point half-ladder could potentially support this notion.

A point against the idea that the numerators can be simplified, however, is the fact that the regular parts that do indeed show up don't actually cause any trouble–or at least,

we suspect that they shouldn't from the few momentum space samples we took. The amplitude as-is is perfectly valid, and will likely even be usable after some (read: a lot of) computational massaging. There is no *need* to simplify the numerators further, as there is no issue with the result per-se. It just becomes a rather messy affair at this height of the interaction, and one would hope that there is some way to simplify the process a bit.

Part III: Conclusion and Acknowledgements

10 Conclusion

We have discussed amplitude construction through both traditional Feynman methods, using Feynman diagrams and rules, and the new, not fully understood, Double Copy, which has been found to tie a growing web of theories together through a somewhat 'ad-hoc' method of constructing amplitudes of one theory through another, or just through an ansatze entirely. In order to probe the Double Copy we set out to calculate DBI amplitudes through both it and traditional Feynman methods, in order to then apply a single-leg soft limit to their interactions to attempt to recover the soft limit cancellation that takes place between the different types of Feynman diagrams used to construct this amplitude. 4 and 6-point DBI amplitudes were constructed and compared yet sadly the 6-point DC amplitude was not found in a usable form due to incomplete factorisation elimination. The 6-point Feynman amplitude *was* properly constructed however, and the soft limit was applied to find the exact set of terms that remain at $\mathcal{O}(\varepsilon)$ when the exchange and contact diagrams are considered separately but cancel out when the contributions of the different types of diagrams are collected in the full amplitude.

The Double Copy amplitude that was found was tested and confirmed to factorise correctly when taking a specific sample of momentum-space coordinates, but the amplitude at large was too hefty to properly reduce to the result found through Feynman methodology. The conclusion was made that the amplitude, as it does factorise correctly, will be capable of reducing to the right form but was caught in mathematical tangles beyond the processing power and methods available to us. A noteworthy property of the different kinds of BCJ diagrams was found, as incorrectly factorising terms appear in both types of diagrams yet the specific momentum space samples showed that their unwanted factorising contributions cancelled out each other exactly.

Even though the results were not refined to the proper form, and as such weren't exactly usable in a general sense, certain projections could be made towards the soft limit applied to the Double Copy. Applying a soft limit is necessarily done after finding the amplitude contributions, and as such one can, to some extent, draw links between the soft limit applied to the Feynman amplitude and that of applying it to the Double Copy amplitude. Assuming that the only difference between the 'tangled' Double Copy amplitude and the neatly factorising Feynman amplitude is a mathematical process of reducing and fitting factorisation terms together, applying the soft limit to one will of course do the same as applying it to the other.

The important query our research did not manage to answer was which terms hail from which diagrams in the Double Copy. The main goal of this research was to see if the soft limit of this theory constructed in the Double Copy would contain the same soft behaviour found through the Feynman method, where both types of diagrams have a lower soft degree than the overall amplitude but cancel out when added together. The options were discussed: On the one hand one might find that the diagrams *do* contain $\sigma = 1$ scaling independently and cancel out. This would, among other things, imply a similarity between the diagram types from the different approaches, and could be quite an interesting result for the Double Copy as a theory. On the other hand one could find the diagrams scale manifestly with $\sigma = 2$ already and as such no cancellation between the types is needed. This would, however, mean that the half-ladder diagrams cancel out their own $\sigma = 1$ contribution, as there *are* terms in the (hard) Lagrangian that scale with $\sigma = 1$,

as we found through Feynman. These terms would then all have to originate from the half-ladder diagrams, as the snowflakes are not capable of exhibiting quartic propagator terms. In this case there *is* still manifest $\sigma = 2$ scaling in both diagrams, but only due to internal cancellation of the half-ladder diagrams. The latter option led us to present an unlikely but curious idea that the snowflake diagrams might serve purely as counterterms to get rid of the unwanted factorisation contributions, implying that the half-ladder diagrams provide all of the terms we find in the Feynman amplitude. Another interpretation of the second option is of course that the snowflake only contributes $\sigma \geq 2$ terms to the (soft) amplitude. More research is needed into these options, likely with more computing power or done by someone with more experience with Mathematica's properties.

As a polar opposite to this last piece of conjecture a potential similarity was proposed between the BCJ diagram structures and the Feynman diagrams relevant to the 6-point interaction. There was found to be a potential similarity between exactly the exchange and half-ladder diagrams, originating from their propagator structure and topological likeness. This conjecture led to a potential significant simplification to the construction of DC numerator terms. Not many conclusions could be found however, and a lot of work would still be needed to properly condense the conjectures presented into a respectable form, as the inability to properly use the DC amplitude left us to present a variety of options rather than confirm, and study, a specific one.

11 Acknowledgements

At the very end of this project there are a few people that deserve thanks. First and foremost of all will be Diederik Roest, the supervisor of this thesis, who has shown inexhaustible patience towards my pace of progress, and has helped me time and again to understand things I suspect should have already been clear to me. I would like to thank him as well for jumping in and offering me this thesis topic when I had some trouble with the prior topic getting off the ground. You have been a great help and I am deeply thankful for that.

The Double Copy is a rather interesting concept, and even though I did not manage to properly apply the soft limit to its result I have found great interest in the subjects I have been studying here.

Another deserved thanks goes out to Dijs de Neeling, who has, among other things, helped me when I was struggling with Mathematica, and has presented interesting papers for consideration in our DC journal club. A similar regard s extended to Sam Veldmeijer, who, together with Diederik and Dijs, was very patient with my inexperience with presenting papers in journal clubs.

A more general thanks is of course directed to everyone who supported me while working on this. My friends and family who gave me kind words and motivated me to keep going, and most of all reminded me that time is finite and deadlines do not budge (much). Thank you all.

One last note of thanks, on the more technical side, goes out to Joshua Ellis, whose Tikz Feyn package made it possible to make the detailed Feynman and BCJ diagrams that appear in this work. More information on this package can be found in [25].

Part IV: Appendix and References

12 Appendix

To illustrate a flavour exchange channel we have depicted below the contribution from the channel with $q_{1,2,3} = p_1 + p_2 + p_3$ exchange momentum:

$$\mathcal{A}_{1,2,3} = \frac{1}{s_{1,2,3}}\Big(s_{1,3}s_{2,3}t_{1,2}(-s_{3,6}s_{4,5}t_{3,6}t_{4,5}+s_{1,5}s_{4,6}t_{3,6}t_{4,5}+s_{2,5}s_{4,6}t_{3,6}t_{4,5}+s_{3,5}s_{4,6}t_{3,6}t_{4,5}$$
$$+s_{1,4}s_{5,6}t_{3,6}t_{4,5}+s_{2,4}s_{5,6}t_{3,6}t_{4,5}+s_{3,4}s_{5,6}t_{3,6}t_{4,5}+s_{3,6}s_{4,5}t_{3,5}t_{4,6}-s_{1,5}s_{4,6}t_{3,5}t_{4,6}-s_{2,5}s_{4,6}t_{3,5}t_{4,6}$$
$$-s_{3,5}s_{4,6}t_{3,5}t_{4,6}+s_{1,4}s_{5,6}t_{3,5}t_{4,6}+s_{2,4}s_{5,6}t_{3,5}t_{4,6}+s_{3,4}s_{5,6}t_{3,5}t_{4,6}+s_{3,6}s_{4,5}t_{3,4}t_{5,6}+s_{1,5}s_{4,6}t_{3,4}t_{5,6}$$
$$+s_{2,5}s_{4,6}t_{3,4}t_{5,6}+s_{3,5}s_{4,6}t_{3,4}t_{5,6}-s_{1,4}s_{5,6}t_{3,4}t_{5,6}-s_{2,4}s_{5,6}t_{3,4}t_{5,6}-s_{3,4}s_{5,6}t_{3,4}t_{5,6}+s_{1,6}s_{4,5}(-t_{3,6}t_{4,5}$$
$$+t_{3,5}t_{4,6}+t_{3,4}t_{5,6})+s_{2,6}s_{4,5}(-t_{3,6}t_{4,5}+t_{3,5}t_{4,6}+t_{3,4}t_{5,6}))+s_{1,2}(s_{1,3}t_{2,3}(-s_{3,6}s_{4,5}t_{1,6}t_{4,5}+s_{1,5}s_{4,6}t_{1,6}t_{4,5}$$
$$+s_{2,5}s_{4,6}t_{1,6}t_{4,5}+s_{3,5}s_{4,6}t_{1,6}t_{4,5}+s_{1,4}s_{5,6}t_{1,6}t_{4,5}+s_{2,4}s_{5,6}t_{1,6}t_{4,5}+s_{3,4}s_{5,6}t_{1,6}t_{4,5}+s_{3,6}s_{4,5}t_{1,5}t_{4,6}$$
$$-s_{1,5}s_{4,6}t_{1,5}t_{4,6}-s_{2,5}s_{4,6}t_{1,5}t_{4,6}-s_{3,5}s_{4,6}t_{1,5}t_{4,6}+s_{1,4}s_{5,6}t_{1,5}t_{4,6}+s_{2,4}s_{5,6}t_{1,5}t_{4,6}+s_{3,4}s_{5,6}t_{1,5}t_{4,6}$$
$$+s_{3,6}s_{4,5}t_{1,4}t_{5,6}+s_{1,5}s_{4,6}t_{1,4}t_{5,6}+s_{2,5}s_{4,6}t_{1,4}t_{5,6}+s_{3,5}s_{4,6}t_{1,4}t_{5,6}-s_{1,4}s_{5,6}t_{1,4}t_{5,6}-s_{2,4}s_{5,6}t_{1,4}t_{5,6}$$
$$-s_{3,4}s_{5,6}t_{1,4}t_{5,6}+s_{1,6}s_{4,5}(-t_{1,6}t_{4,5}+t_{1,5}t_{4,6}+t_{1,4}t_{5,6})+s_{2,6}s_{4,5}(-t_{1,6}t_{4,5}+t_{1,5}t_{4,6}+t_{1,4}t_{5,6}))$$
$$+s_{2,3}t_{1,3}(-s_{3,6}s_{4,5}t_{2,6}t_{4,5}+s_{1,5}s_{4,6}t_{2,6}t_{4,5}+s_{2,5}s_{4,6}t_{2,6}t_{4,5}+s_{3,5}s_{4,6}t_{2,6}t_{4,5}+s_{1,4}s_{5,6}t_{2,6}t_{4,5}$$
$$+s_{2,4}s_{5,6}t_{2,6}t_{4,5}+s_{3,4}s_{5,6}t_{2,6}t_{4,5}+s_{3,6}s_{4,5}t_{2,5}t_{4,6}-s_{1,5}s_{4,6}t_{2,5}t_{4,6}-s_{2,5}s_{4,6}t_{2,5}t_{4,6}-s_{3,5}s_{4,6}t_{2,5}t_{4,6}$$
$$+s_{1,4}s_{5,6}t_{2,5}t_{4,6}+s_{2,4}s_{5,6}t_{2,5}t_{4,6}+s_{3,4}s_{5,6}t_{2,5}t_{4,6}+s_{3,6}s_{4,5}t_{2,4}t_{5,6}+s_{1,5}s_{4,6}t_{2,4}t_{5,6}+s_{2,5}s_{4,6}t_{2,4}t_{5,6}$$
$$+s_{3,5}s_{4,6}t_{2,4}t_{5,6}-s_{1,4}s_{5,6}t_{2,4}t_{5,6}-s_{2,4}s_{5,6}t_{2,4}t_{5,6}-s_{3,4}s_{5,6}t_{2,4}t_{5,6}+s_{1,6}s_{4,5}(-t_{2,6}t_{4,5}+t_{2,5}t_{4,6}+t_{2,4}t_{5,6})$$
$$+ s_{2,6}s_{4,5}(-t_{2,6}t_{4,5} + t_{2,5}t_{4,6} + t_{2,4}t_{5,6})))\Big) \quad (80)$$

The full version of the compact kinematic numerator found in [2] is given as follows:

$$\begin{aligned}
N_{a,b,c,d,e,f} = s_{a,b}\big(&-s_{e,f}\left(s_{b,c}\left(-4s_{a,f}+4\left(s_{b,d}+s_{c,d}+s_{c,e}\right)+5s_{d,e}\right)\right.\\
&+s_{a,c}\left(-4s_{a,f}+4\left(s_{b,d}+s_{c,d}\right)+s_{b,c}+9s_{d,e}\right)+4s_{a,b}^2+5s_{a,c}s_{a,d}+s_{a,c}^2\big)\\
&+4\left(s_{a,b}+s_{a,c}+s_{b,c}\right)\left(\left(s_{a,c}+s_{b,c}\right)\left(-s_{a,f}+s_{b,c}+s_{b,d}+s_{c,d}\right)+s_{b,c}s_{c,e}\right)\\
&-4s_{d,e}\left(s_{a,d}s_{b,c}+s_{a,c}\left(s_{b,d}+s_{c,d}\right)\right)+s_{e,f}^2\left(4s_{a,b}+5s_{a,c}\right)\big)\\
&+s_{f,e}\left(-s_{b,a}\left(s_{f,d}\left(-4s_{f,a}+9s_{c,b}+4\left(s_{d,c}+s_{e,c}\right)+s_{e,d}\right)\right.\right.\\
&+s_{e,d}\left(-4s_{f,a}+4\left(s_{d,b}+s_{d,c}+s_{e,c}\right)+5s_{c,b}\right)+5s_{f,c}s_{f,d}+s_{f,d}^2+4s_{f,e}^2\big)\\
&+4\left(s_{e,d}+s_{f,d}+s_{f,e}\right)\left(\left(s_{e,d}+s_{f,d}\right)\left(-s_{f,a}+s_{d,c}+s_{e,c}+s_{e,d}\right)+s_{d,b}s_{e,d}\right)\\
&+s_{b,a}^2\left(5s_{f,d}+4s_{f,e}\right)-4s_{c,b}\left(s_{f,c}s_{e,d}+s_{f,d}\left(s_{d,c}+s_{e,c}\right)\right)\big)
\end{aligned} \quad (81)$$

Full $A_{12,34,56}$ in only 9 indep Mandelstams: $s_{1,2}, s_{1,3}, s_{1,4}, s_{1,5}, s_{2,3}, s_{2,4}, s_{3,4}, s_{3,5}, s_{4,5}$

$$
\begin{aligned}
&\frac{4s_{1,4}s_{1,3}^3}{s_{1,3}+s_{1,4}+s_{3,4}} - \frac{4s_{4,5}^2 s_{1,3}^3}{(s_{1,2}+s_{1,3}+s_{2,3})(s_{1,3}+s_{1,4}+s_{3,4})} - 4s_{1,4}s_{1,3}^2 \\
&+ \frac{8s_{1,4}s_{3,5}s_{1,3}^2}{s_{1,3}+s_{1,4}+s_{3,4}} + 4s_{3,5}s_{1,3}^2 + \frac{8s_{1,4}s_{4,5}s_{1,3}^2}{s_{1,3}+s_{1,4}+s_{3,4}} - 4s_{4,5}s_{1,3}^2 \\
&+ \frac{8s_{1,4}^2 s_{1,3}^2}{s_{1,3}+s_{1,4}+s_{3,4}} + \frac{4s_{1,2}s_{1,4}s_{1,3}^2}{s_{1,3}+s_{1,4}+s_{3,4}} + \frac{8s_{1,4}s_{1,5}s_{1,3}^2}{s_{1,3}+s_{1,4}+s_{3,4}} + \frac{4s_{1,4}s_{2,3}s_{1,3}^2}{s_{1,3}+s_{1,4}+s_{3,4}} \\
&+ \frac{4s_{1,4}s_{2,4}s_{1,3}^2}{s_{1,3}+s_{1,4}+s_{3,4}} + \frac{8s_{1,4}s_{3,4}s_{1,3}^2}{s_{1,3}+s_{1,4}+s_{3,4}} - \frac{4s_{1,2}s_{4,5}^2 s_{1,3}^2}{(s_{1,2}+s_{1,3}+s_{2,3})(s_{1,3}+s_{1,4}+s_{3,4})} \\
&- \frac{4s_{3,4}s_{4,5}^2 s_{1,3}^2}{(s_{1,2}+s_{1,3}+s_{2,3})(s_{1,3}+s_{1,4}+s_{3,4})} - \frac{4s_{3,5}^2 s_{1,3}^2}{s_{3,4}+s_{3,5}+s_{4,5}} \\
&- \frac{4s_{3,4}s_{3,5}s_{1,3}^2}{s_{3,4}+s_{3,5}+s_{4,5}} + \frac{4s_{1,5}^2 s_{1,3}^2}{s_{1,3}+s_{1,4}+s_{2,3}+s_{2,4}+s_{3,4}+s_{3,5}+s_{4,5}} \\
&+ \frac{4s_{1,2}s_{1,5}s_{1,3}^2}{s_{1,3}+s_{1,4}+s_{2,3}+s_{2,4}+s_{3,4}+s_{3,5}+s_{4,5}} - 4s_{1,4}^2 s_{1,3} - 4s_{1,5}^2 s_{1,3} \\
&+ \frac{4s_{1,4}s_{3,5}^2 s_{1,3}}{s_{1,3}+s_{1,4}+s_{3,4}} + \frac{4s_{1,4}s_{2,3}s_{4,5}^2 s_{1,3}}{(s_{1,2}+s_{1,3}+s_{2,3})(s_{1,3}+s_{1,4}+s_{3,4})} - 4s_{1,2}s_{1,4}s_{1,3} \\
&- 4s_{1,2}s_{1,5}s_{1,3} - 8s_{1,4}s_{1,5}s_{1,3} - 4s_{1,4}s_{2,3}s_{1,3} - 4s_{1,4}s_{2,4}s_{1,3} - 4s_{1,5}s_{2,4}s_{1,3} \\
&- 4s_{1,4}s_{3,4}s_{1,3} + 4s_{1,2}s_{3,5}s_{1,3} + 8s_{1,5}s_{3,5}s_{1,3} + \frac{4s_{1,4}s_{2,4}s_{3,5}s_{1,3}}{s_{1,2}+s_{1,4}+s_{2,4}} \\
&+ \frac{8s_{1,4}^2 s_{3,5}s_{1,3}}{s_{1,3}+s_{1,4}+s_{3,4}} + \frac{4s_{1,2}s_{1,4}s_{3,5}s_{1,3}}{s_{1,3}+s_{1,4}+s_{3,4}} + \frac{8s_{1,4}s_{1,5}s_{3,5}s_{1,3}}{s_{1,3}+s_{1,4}+s_{3,4}} + \frac{4s_{1,4}s_{2,3}s_{3,5}s_{1,3}}{s_{1,3}+s_{1,4}+s_{3,4}} \\
&+ \frac{4s_{1,4}s_{2,4}s_{3,5}s_{1,3}}{s_{1,3}+s_{1,4}+s_{3,4}} + \frac{8s_{1,4}s_{3,4}s_{3,5}s_{1,3}}{s_{1,3}+s_{1,4}+s_{3,4}} - 4s_{1,2}s_{4,5}s_{1,3} - 8s_{1,4}s_{4,5}s_{1,3} \\
&- 8s_{1,5}s_{4,5}s_{1,3} + \frac{4s_{2,3}s_{2,4}s_{4,5}s_{1,3}}{s_{1,2}+s_{1,3}+s_{2,3}} - 4s_{2,4}s_{4,5}s_{1,3} + \frac{4s_{2,3}s_{3,4}s_{4,5}s_{1,3}}{s_{1,2}+s_{1,3}+s_{2,3}} \\
&- 4s_{3,4}s_{4,5}s_{1,3} + \frac{8s_{1,4}s_{3,5}s_{4,5}s_{1,3}}{s_{1,3}+s_{1,4}+s_{3,4}} + \frac{4s_{1,4}s_{2,3}s_{4,5}s_{1,3}}{s_{1,2}+s_{1,3}+s_{2,3}} + \frac{8s_{1,4}^2 s_{4,5}s_{1,3}}{s_{1,3}+s_{1,4}+s_{3,4}} \\
&+ \frac{4s_{1,2}s_{1,4}s_{4,5}s_{1,3}}{s_{1,3}+s_{1,4}+s_{3,4}} + \frac{8s_{1,4}s_{1,5}s_{4,5}s_{1,3}}{s_{1,3}+s_{1,4}+s_{3,4}} + \frac{4s_{1,4}s_{2,3}s_{4,5}s_{1,3}}{s_{1,3}+s_{1,4}+s_{3,4}} + \frac{4s_{1,4}s_{2,4}s_{4,5}s_{1,3}}{s_{1,3}+s_{1,4}+s_{3,4}} \\
&+ \frac{8s_{1,4}s_{3,4}s_{4,5}s_{1,3}}{s_{1,3}+s_{1,4}+s_{3,4}} + \frac{4s_{1,4}^3 s_{1,3}}{s_{1,3}+s_{1,4}+s_{3,4}} + \frac{4s_{1,2}s_{1,4}^2 s_{1,3}}{s_{1,3}+s_{1,4}+s_{3,4}} + \frac{4s_{1,4}s_{1,5}^2 s_{1,3}}{s_{1,3}+s_{1,4}+s_{3,4}} \\
&+ \frac{4s_{1,4}s_{3,4}^2 s_{1,3}}{s_{1,3}+s_{1,4}+s_{3,4}} + \frac{8s_{1,4}^2 s_{1,5}s_{1,3}}{s_{1,3}+s_{1,4}+s_{3,4}} + \frac{4s_{1,2}s_{1,4}s_{1,5}s_{1,3}}{s_{1,3}+s_{1,4}+s_{3,4}} + \frac{4s_{1,4}^2 s_{2,3}s_{1,3}}{s_{1,3}+s_{1,4}+s_{3,4}} \\
&+ \frac{4s_{1,4}s_{1,5}s_{2,3}s_{1,3}}{s_{1,3}+s_{1,4}+s_{3,4}} + \frac{4s_{1,4}^2 s_{2,4}s_{1,3}}{s_{1,3}+s_{1,4}+s_{3,4}} + \frac{4s_{1,4}s_{1,5}s_{2,4}s_{1,3}}{s_{1,3}+s_{1,4}+s_{3,4}} + \frac{8s_{1,4}^2 s_{3,4}s_{1,3}}{s_{1,3}+s_{1,4}+s_{3,4}} \\
&+ \frac{4s_{1,2}s_{1,4}s_{3,4}s_{1,3}}{s_{1,3}+s_{1,4}+s_{3,4}} + \frac{8s_{1,4}s_{1,5}s_{3,4}s_{1,3}}{s_{1,3}+s_{1,4}+s_{3,4}} + \frac{4s_{1,4}s_{2,3}s_{3,4}s_{1,3}}{s_{1,3}+s_{1,4}+s_{3,4}} + \frac{4s_{1,4}s_{2,4}s_{3,4}s_{1,3}}{s_{1,3}+s_{1,4}+s_{3,4}} \\
&- \frac{4s_{1,2}s_{3,4}s_{4,5}^2 s_{1,3}}{(s_{1,2}+s_{1,3}+s_{2,3})(s_{1,3}+s_{1,4}+s_{3,4})} + \frac{4s_{1,5}s_{2,3}s_{2,4}s_{1,3}}{s_{2,3}+s_{2,4}+s_{3,4}} - \frac{4s_{1,2}s_{3,5}^2 s_{1,3}}{s_{3,4}+s_{3,5}+s_{4,5}} \\
&- \frac{8s_{1,4}s_{3,5}^2 s_{1,3}}{s_{3,4}+s_{3,5}+s_{4,5}} - \frac{8s_{1,5}s_{3,5}^2 s_{1,3}}{s_{3,4}+s_{3,5}+s_{4,5}} - \frac{4s_{1,2}s_{3,4}s_{3,5}s_{1,3}}{s_{3,4}+s_{3,5}+s_{4,5}} - \frac{8s_{1,4}s_{3,4}s_{3,5}s_{1,3}}{s_{3,4}+s_{3,5}+s_{4,5}} \\
&- \frac{8s_{1,5}s_{3,4}s_{3,5}s_{1,3}}{s_{3,4}+s_{3,5}+s_{4,5}} + \frac{8s_{1,5}^2 s_{2,3}s_{1,3}}{s_{1,3}+s_{1,4}+s_{2,3}+s_{2,4}+s_{3,4}+s_{3,5}+s_{4,5}} + \text{next page}
\end{aligned}
\tag{82}
$$

$$+\frac{8s_{1,2}s_{1,5}s_{2,3}s_{1,3}}{s_{1,3}+s_{1,4}+s_{2,3}+s_{2,4}+s_{3,4}+s_{3,5}+s_{4,5}}+\frac{4s_{1,5}^2s_{3,4}s_{1,3}}{s_{1,3}+s_{1,4}+s_{2,3}+s_{2,4}+s_{3,4}+s_{3,5}+s_{4,5}}$$

$$+\frac{4s_{1,2}s_{1,5}s_{3,4}s_{1,3}}{s_{1,3}+s_{1,4}+s_{2,3}+s_{2,4}+s_{3,4}+s_{3,5}+s_{4,5}}+\frac{8s_{1,5}^2s_{3,5}s_{1,3}}{s_{1,3}+s_{1,4}+s_{2,3}+s_{2,4}+s_{3,4}+s_{3,5}+s_{4,5}}$$

$$+\frac{8s_{1,2}s_{1,5}s_{3,5}s_{1,3}}{s_{1,3}+s_{1,4}+s_{2,3}+s_{2,4}+s_{3,4}+s_{3,5}+s_{4,5}}-4s_{1,4}s_{3,5}^2+\frac{4s_{1,4}s_{2,4}s_{3,5}^2}{s_{1,2}+s_{1,4}+s_{2,4}}-4s_{1,5}^2s_{2,3}$$

$$-4s_{1,2}s_{1,5}s_{2,3}-4s_{1,4}s_{1,5}s_{2,3}-4s_{1,4}s_{2,3}s_{3,5}-4s_{1,4}s_{3,4}s_{3,5}+\frac{4s_{1,4}s_{2,4}s_{3,4}s_{3,5}}{s_{1,2}+s_{1,4}+s_{2,4}}$$

$$+\frac{4s_{1,4}s_{2,3}s_{2,4}s_{3,5}}{s_{1,2}+s_{1,4}+s_{2,4}}+\frac{4s_{1,5}^2s_{2,3}s_{2,4}}{s_{2,3}+s_{2,4}+s_{3,4}}+\frac{4s_{1,2}s_{1,5}s_{2,3}s_{2,4}}{s_{2,3}+s_{2,4}+s_{3,4}}+\frac{4s_{1,4}s_{1,5}s_{2,3}s_{2,4}}{s_{2,3}+s_{2,4}+s_{3,4}}-\frac{4s_{1,4}^2s_{3,5}^2}{s_{3,4}+s_{3,5}+s_{4,5}}$$

$$-\frac{4s_{1,5}^2s_{3,5}^2}{s_{3,4}+s_{3,5}+s_{4,5}}-\frac{4s_{1,2}s_{1,4}s_{3,5}^2}{s_{3,4}+s_{3,5}+s_{4,5}}-\frac{4s_{1,2}s_{1,5}s_{3,5}^2}{s_{3,4}+s_{3,5}+s_{4,5}}-\frac{8s_{1,4}s_{1,5}s_{3,5}^2}{s_{3,4}+s_{3,5}+s_{4,5}}$$

$$-\frac{4s_{1,4}^2s_{3,4}s_{3,5}}{s_{3,4}+s_{3,5}+s_{4,5}}-\frac{4s_{1,5}^2s_{3,4}s_{3,5}}{s_{3,4}+s_{3,5}+s_{4,5}}-\frac{4s_{1,2}s_{1,4}s_{3,4}s_{3,5}}{s_{3,4}+s_{3,5}+s_{4,5}}-\frac{4s_{1,2}s_{1,5}s_{3,4}s_{3,5}}{s_{3,4}+s_{3,5}+s_{4,5}}-\frac{8s_{1,4}s_{1,5}s_{3,4}s_{3,5}}{s_{3,4}+s_{3,5}+s_{4,5}}$$

$$+\frac{4s_{1,5}^2s_{2,3}^2}{s_{1,3}+s_{1,4}+s_{2,3}+s_{2,4}+s_{3,4}+s_{3,5}+s_{4,5}}+\frac{4s_{1,2}s_{1,5}s_{2,3}^2}{s_{1,3}+s_{1,4}+s_{2,3}+s_{2,4}+s_{3,4}+s_{3,5}+s_{4,5}}$$

$$+\frac{4s_{1,5}^2s_{3,5}^2}{s_{1,3}+s_{1,4}+s_{2,3}+s_{2,4}+s_{3,4}+s_{3,5}+s_{4,5}}+\frac{4s_{1,2}s_{1,5}s_{3,5}^2}{s_{1,3}+s_{1,4}+s_{2,3}+s_{2,4}+s_{3,4}+s_{3,5}+s_{4,5}}$$

$$+\frac{4s_{1,5}^2s_{2,3}s_{3,4}}{s_{1,3}+s_{1,4}+s_{2,3}+s_{2,4}+s_{3,4}+s_{3,5}+s_{4,5}}+\frac{4s_{1,2}s_{1,5}s_{2,3}s_{3,4}}{s_{1,3}+s_{1,4}+s_{2,3}+s_{2,4}+s_{3,4}+s_{3,5}+s_{4,5}}$$

$$+\frac{8s_{1,5}^2s_{2,3}s_{3,5}}{s_{1,3}+s_{1,4}+s_{2,3}+s_{2,4}+s_{3,4}+s_{3,5}+s_{4,5}}+\frac{8s_{1,2}s_{1,5}s_{2,3}s_{3,5}}{s_{1,3}+s_{1,4}+s_{2,3}+s_{2,4}+s_{3,4}+s_{3,5}+s_{4,5}}$$

$$+\frac{4s_{1,5}^2s_{3,4}s_{3,5}}{s_{1,3}+s_{1,4}+s_{2,3}+s_{2,4}+s_{3,4}+s_{3,5}+s_{4,5}}+\frac{4s_{1,2}s_{1,5}s_{3,4}s_{3,5}}{s_{1,3}+s_{1,4}+s_{2,3}+s_{2,4}+s_{3,4}+s_{3,5}+s_{4,5}}$$

$A_{12,34,56}$ in Mandelstam invariant form with Soft Limit θ:

$$\frac{4s_{1,3}s_{1,4}^3\theta^4}{\theta s_{1,3}+\theta s_{1,4}+s_{3,4}}+\frac{8s_{1,3}^2s_{1,4}^2\theta^4}{\theta s_{1,3}+\theta s_{1,4}+s_{3,4}}+\frac{4s_{1,2}s_{1,3}s_{1,4}^2\theta^4}{\theta s_{1,3}+\theta s_{1,4}+s_{3,4}}+\frac{4s_{1,3}s_{1,4}s_{1,5}^2\theta^4}{\theta s_{1,3}+\theta s_{1,4}+s_{3,4}}$$

$$+\frac{4s_{1,3}^3s_{1,4}\theta^4}{\theta s_{1,3}+\theta s_{1,4}+s_{3,4}}+\frac{4s_{1,2}s_{1,3}^2s_{1,4}\theta^4}{\theta s_{1,3}+\theta s_{1,4}+s_{3,4}}+\frac{8s_{1,3}s_{1,4}^2s_{1,5}\theta^4}{\theta s_{1,3}+\theta s_{1,4}+s_{3,4}}+\frac{8s_{1,3}^2s_{1,4}s_{1,5}\theta^4}{\theta s_{1,3}+\theta s_{1,4}+s_{3,4}}$$

$$+\frac{4s_{1,2}s_{1,3}s_{1,4}s_{1,5}\theta^4}{\theta s_{1,3}+\theta s_{1,4}+s_{3,4}}+\frac{4s_{1,3}^2s_{1,5}^2\theta^4}{\theta s_{1,3}+\theta s_{1,4}+s_{3,5}+s_{4,5}+s_{2,3,4}}+\frac{4s_{1,2}s_{1,3}^2s_{1,5}\theta^4}{\theta s_{1,3}+\theta s_{1,4}+s_{3,5}+s_{4,5}+s_{2,3,4}}$$

$$-4s_{1,3}s_{1,4}^2\theta^3-4s_{1,3}s_{1,5}^2\theta^3-4s_{1,3}^2s_{1,4}\theta^3-4s_{1,2}s_{1,3}s_{1,4}\theta^3-4s_{1,2}s_{1,3}s_{1,5}\theta^3-8s_{1,3}s_{1,4}s_{1,5}\theta^3$$

$$+\frac{8s_{1,3}s_{1,4}^2s_{3,5}\theta^3}{\theta s_{1,3}+\theta s_{1,4}+s_{3,4}}+\frac{8s_{1,3}^2s_{1,4}s_{3,5}\theta^3}{\theta s_{1,3}+\theta s_{1,4}+s_{3,4}}+\frac{4s_{1,2}s_{1,3}s_{1,4}s_{3,5}\theta^3}{\theta s_{1,3}+\theta s_{1,4}+s_{3,4}}+\frac{8s_{1,3}s_{1,4}s_{1,5}s_{3,5}\theta^3}{\theta s_{1,3}+\theta s_{1,4}+s_{3,4}}$$

$$+\frac{8s_{1,3}s_{1,4}^2s_{4,5}\theta^3}{\theta s_{1,3}+\theta s_{1,4}+s_{3,4}}+\frac{8s_{1,3}^2s_{1,4}s_{4,5}\theta^3}{\theta s_{1,3}+\theta s_{1,4}+s_{3,4}}+\frac{4s_{1,2}s_{1,3}s_{1,4}s_{4,5}\theta^3}{\theta s_{1,3}+\theta s_{1,4}+s_{3,4}}+\frac{8s_{1,3}s_{1,4}s_{1,5}s_{4,5}\theta^3}{\theta s_{1,3}+\theta s_{1,4}+s_{3,4}}$$

$$+\frac{4s_{1,3}s_{1,4}^2s_{2,3}\theta^3}{\theta s_{1,3}+\theta s_{1,4}+s_{3,4}}+\frac{4s_{1,3}^2s_{1,4}s_{2,3}\theta^3}{\theta s_{1,3}+\theta s_{1,4}+s_{3,4}}+\frac{4s_{1,3}s_{1,4}s_{1,5}s_{2,3}\theta^3}{\theta s_{1,3}+\theta s_{1,4}+s_{3,4}}+\frac{4s_{1,3}s_{1,4}^2s_{2,4}\theta^3}{\theta s_{1,3}+\theta s_{1,4}+s_{3,4}}$$

$$+\frac{4s_{1,3}^2s_{1,4}s_{2,4}\theta^3}{\theta s_{1,3}+\theta s_{1,4}+s_{3,4}}+\frac{4s_{1,3}s_{1,4}s_{1,5}s_{2,4}\theta^3}{\theta s_{1,3}+\theta s_{1,4}+s_{3,4}}+\frac{8s_{1,3}s_{1,4}^2s_{3,4}\theta^3}{\theta s_{1,3}+\theta s_{1,4}+s_{3,4}}+\frac{8s_{1,3}^2s_{1,4}s_{3,4}\theta^3}{\theta s_{1,3}+\theta s_{1,4}+s_{3,4}}$$

$$+\frac{4s_{1,2}s_{1,3}s_{1,4}s_{3,4}\theta^3}{\theta s_{1,3}+\theta s_{1,4}+s_{3,4}}+\frac{8s_{1,3}s_{1,4}s_{1,5}s_{3,4}\theta^3}{\theta s_{1,3}+\theta s_{1,4}+s_{3,4}}-\frac{4s_{1,3}^3s_{4,5}^2\theta^3}{(\theta s_{1,2}+\theta s_{1,3}+s_{2,3})(\theta s_{1,3}+\theta s_{1,4}+s_{3,4})}+\text{next page} \tag{83}$$

$$
\begin{aligned}
&- \frac{4s_{1,2}s_{1,3}^2s_{4,5}^2\theta^3}{\left(\theta s_{1,2}+\theta s_{1,3}+s_{2,3}\right)\left(\theta s_{1,3}+\theta s_{1,4}+s_{3,4}\right)} + \frac{8s_{1,3}s_{1,5}^2s_{2,3}\theta^3}{\theta s_{1,3}+\theta s_{1,4}+s_{3,5}+s_{4,5}+s_{2,3,4}} \\
&+ \frac{8s_{1,2}s_{1,3}s_{1,5}s_{2,3}\theta^3}{\theta s_{1,3}+\theta s_{1,4}+s_{3,5}+s_{4,5}+s_{2,3,4}} + \frac{4s_{1,3}s_{1,5}^2s_{3,4}\theta^3}{\theta s_{1,3}+\theta s_{1,4}+s_{3,5}+s_{4,5}+s_{2,3,4}} \\
&+ \frac{4s_{1,2}s_{1,3}s_{1,5}s_{3,4}\theta^3}{\theta s_{1,3}+\theta s_{1,4}+s_{3,5}+s_{4,5}+s_{2,3,4}} + \frac{8s_{1,3}s_{1,5}^2s_{3,5}\theta^3}{\theta s_{1,3}+\theta s_{1,4}+s_{3,5}+s_{4,5}+s_{2,3,4}} \\
&+ \frac{8s_{1,2}s_{1,3}s_{1,5}s_{3,5}\theta^3}{\theta s_{1,3}+\theta s_{1,4}+s_{3,5}+s_{4,5}+s_{2,3,4}} + \frac{4s_{1,3}s_{1,4}s_{3,5}^2\theta^2}{\theta s_{1,3}+\theta s_{1,4}+s_{3,4}} \\
&+ \frac{4s_{1,3}s_{1,4}s_{2,3}s_{4,5}^2\theta^2}{\left(\theta s_{1,2}+\theta s_{1,3}+s_{2,3}\right)\left(\theta s_{1,3}+\theta s_{1,4}+s_{3,4}\right)} - 4s_{1,5}^2s_{2,3}\theta^2 - 4s_{1,3}s_{1,4}s_{2,3}\theta^2 \\
&- 4s_{1,2}s_{1,5}s_{2,3}\theta^2 - 4s_{1,4}s_{1,5}s_{2,3}\theta^2 - 4s_{1,3}s_{1,4}s_{2,4}\theta^2 - 4s_{1,3}s_{1,5}s_{2,4}\theta^2 - 4s_{1,3}s_{1,4}s_{3,4}\theta^2 \\
&+ 4s_{1,3}^2s_{3,5}\theta^2 + 4s_{1,2}s_{1,3}s_{3,5}\theta^2 + 8s_{1,3}s_{1,5}s_{3,5}\theta^2 + \frac{4s_{1,3}s_{1,4}s_{2,4}s_{3,5}\theta^2}{\theta s_{1,2}+\theta s_{1,4}+s_{2,4}} \\
&+ \frac{4s_{1,3}s_{1,4}s_{2,3}s_{3,5}\theta^2}{\theta s_{1,3}+\theta s_{1,4}+s_{3,4}} + \frac{4s_{1,3}s_{1,4}s_{2,4}s_{3,5}\theta^2}{\theta s_{1,3}+\theta s_{1,4}+s_{3,4}} + \frac{8s_{1,3}s_{1,4}s_{3,4}s_{3,5}\theta^2}{\theta s_{1,3}+\theta s_{1,4}+s_{3,4}} - 4s_{1,3}^2s_{4,5}\theta^2 \\
&- 4s_{1,2}s_{1,3}s_{4,5}\theta^2 - 8s_{1,3}s_{1,4}s_{4,5}\theta^2 - 8s_{1,3}s_{1,5}s_{4,5}\theta^2 + \frac{8s_{1,3}s_{1,4}s_{3,5}s_{4,5}\theta^2}{\theta s_{1,3}+\theta s_{1,4}+s_{3,4}} \\
&+ \frac{4s_{1,3}s_{1,4}s_{2,3}s_{4,5}\theta^2}{\theta s_{1,2}+\theta s_{1,3}+s_{2,3}} + \frac{4s_{1,3}s_{1,4}s_{2,3}s_{4,5}\theta^2}{\theta s_{1,3}+\theta s_{1,4}+s_{3,4}} + \frac{4s_{1,3}s_{1,4}s_{2,4}s_{4,5}\theta^2}{\theta s_{1,3}+\theta s_{1,4}+s_{3,4}} \\
&+ \frac{8s_{1,3}s_{1,4}s_{3,4}s_{4,5}\theta^2}{\theta s_{1,3}+\theta s_{1,4}+s_{3,4}} + \frac{4s_{1,3}s_{1,4}s_{3,4}^2\theta^2}{\theta s_{1,3}+\theta s_{1,4}+s_{3,4}} + \frac{4s_{1,3}s_{1,4}s_{2,3}s_{3,4}\theta^2}{\theta s_{1,3}+\theta s_{1,4}+s_{3,4}} \\
&+ \frac{4s_{1,3}s_{1,4}s_{2,4}s_{3,4}\theta^2}{\theta s_{1,3}+\theta s_{1,4}+s_{3,4}} - \frac{4s_{1,3}^2s_{3,4}s_{4,5}^2\theta^2}{\left(\theta s_{1,2}+\theta s_{1,3}+s_{2,3}\right)\left(\theta s_{1,3}+\theta s_{1,4}+s_{3,4}\right)} \\
&- \frac{4s_{1,2}s_{1,3}s_{3,4}s_{4,5}^2\theta^2}{\left(\theta s_{1,2}+\theta s_{1,3}+s_{2,3}\right)\left(\theta s_{1,3}+\theta s_{1,4}+s_{3,4}\right)} + \frac{4s_{1,5}^2s_{2,3}s_{2,4}\theta^2}{s_{2,3,4}} \\
&+ \frac{4s_{1,2}s_{1,5}s_{2,3}s_{2,4}\theta^2}{s_{2,3,4}} + \frac{4s_{1,3}s_{1,5}s_{2,3}s_{2,4}\theta^2}{s_{2,3,4}} + \frac{4s_{1,4}s_{1,5}s_{2,3}s_{2,4}\theta^2}{s_{2,3,4}} \\
&+ \frac{4s_{1,5}^2s_{2,3}^2\theta^2}{\theta s_{1,3}+\theta s_{1,4}+s_{3,5}+s_{4,5}+s_{2,3,4}} + \frac{4s_{1,2}s_{1,5}s_{2,3}^2\theta^2}{\theta s_{1,3}+\theta s_{1,4}+s_{3,5}+s_{4,5}+s_{2,3,4}} \\
&+ \frac{4s_{1,5}^2s_{3,5}^2\theta^2}{\theta s_{1,3}+\theta s_{1,4}+s_{3,5}+s_{4,5}+s_{2,3,4}} + \frac{4s_{1,2}s_{1,5}s_{3,5}^2\theta^2}{\theta s_{1,3}+\theta s_{1,4}+s_{3,5}+s_{4,5}+s_{2,3,4}} \\
&+ \frac{4s_{1,5}^2s_{2,3}s_{3,4}\theta^2}{\theta s_{1,3}+\theta s_{1,4}+s_{3,5}+s_{4,5}+s_{2,3,4}} + \frac{4s_{1,2}s_{1,5}s_{2,3}s_{3,4}\theta^2}{\theta s_{1,3}+\theta s_{1,4}+s_{3,5}+s_{4,5}+s_{2,3,4}} \\
&+ \frac{8s_{1,5}^2s_{2,3}s_{3,5}\theta^2}{\theta s_{1,3}+\theta s_{1,4}+s_{3,5}+s_{4,5}+s_{2,3,4}} + \frac{8s_{1,2}s_{1,5}s_{2,3}s_{3,5}\theta^2}{\theta s_{1,3}+\theta s_{1,4}+s_{3,5}+s_{4,5}+s_{2,3,4}} \\
&+ \frac{4s_{1,5}^2s_{3,4}s_{3,5}\theta^2}{\theta s_{1,3}+\theta s_{1,4}+s_{3,5}+s_{4,5}+s_{2,3,4}} + \frac{4s_{1,2}s_{1,5}s_{3,4}s_{3,5}\theta^2}{\theta s_{1,3}+\theta s_{1,4}+s_{3,5}+s_{4,5}+s_{2,3,4}} \\
&- \frac{4s_{1,3}^2s_{3,5}^2\theta^2}{s_{3,4,5}} - \frac{4s_{1,4}^2s_{3,5}^2\theta^2}{s_{3,4,5}} - \frac{4s_{1,5}^2s_{3,5}^2\theta^2}{s_{3,4,5}} - \frac{4s_{1,2}s_{1,3}s_{3,5}^2\theta^2}{s_{3,4,5}} - \frac{4s_{1,2}s_{1,4}s_{3,5}^2\theta^2}{s_{3,4,5}} \\
&- \frac{8s_{1,3}s_{1,4}s_{3,5}^2\theta^2}{s_{3,4,5}} - \frac{4s_{1,2}s_{1,5}s_{3,5}^2\theta^2}{s_{3,4,5}} - \frac{8s_{1,3}s_{1,5}s_{3,5}^2\theta^2}{s_{3,4,5}} - \frac{8s_{1,4}s_{1,5}s_{3,5}^2\theta^2}{s_{3,4,5}} \\
&- \frac{4s_{1,3}^2s_{3,4}s_{3,5}\theta^2}{s_{3,4,5}} - \frac{4s_{1,4}^2s_{3,4}s_{3,5}\theta^2}{s_{3,4,5}} - \frac{4s_{1,5}^2s_{3,4}s_{3,5}\theta^2}{s_{3,4,5}} - \frac{4s_{1,2}s_{1,3}s_{3,4}s_{3,5}\theta^2}{s_{3,4,5}} \\
&- \frac{4s_{1,2}s_{1,4}s_{3,4}s_{3,5}\theta^2}{s_{3,4,5}} - \frac{8s_{1,3}s_{1,4}s_{3,4}s_{3,5}\theta^2}{s_{3,4,5}} - \frac{4s_{1,2}s_{1,5}s_{3,4}s_{3,5}\theta^2}{s_{3,4,5}} \\
&- \frac{8s_{1,3}s_{1,5}s_{3,4}s_{3,5}\theta^2}{s_{3,4,5}} - \frac{8s_{1,4}s_{1,5}s_{3,4}s_{3,5}\theta^2}{s_{3,4,5}} - 4s_{1,4}s_{3,5}^2\theta + \frac{4s_{1,4}s_{2,4}s_{3,5}^2\theta}{\theta s_{1,2}+\theta s_{1,4}+s_{2,4}} \\
&- 4s_{1,4}s_{2,3}s_{3,5}\theta - 4s_{1,4}s_{3,4}s_{3,5}\theta + \frac{4s_{1,4}s_{2,4}s_{3,4}s_{3,5}\theta}{\theta s_{1,2}+\theta s_{1,4}+s_{2,4}} + \frac{4s_{1,4}s_{2,3}s_{2,4}s_{3,5}\theta}{\theta s_{1,2}+\theta s_{1,4}+s_{2,4}} \\
&- 4s_{1,3}s_{2,4}s_{4,5}\theta + \frac{4s_{1,3}s_{2,3}s_{2,4}s_{4,5}\theta}{\theta s_{1,2}+\theta s_{1,3}+s_{2,3}} - 4s_{1,3}s_{3,4}s_{4,5}\theta + \frac{4s_{1,3}s_{2,3}s_{3,4}s_{4,5}\theta}{\theta s_{1,2}+\theta s_{1,3}+s_{2,3}}
\end{aligned}
$$

Apalogies for the formatting, it was hard to get an equation as large as this to fit nicely.

References

[1] Zvi Bern, John Joseph Carrasco, Marco Chiodaroli, Henrik Johansson, and Radu Roiban. The Duality Between Color and Kinematics and its Applications. 9 2019. arXiv:1909.01358.

[2] Dijs de Neeling, Diederik Roest, and Sam Veldmeijer. Flavour-kinematic duality for Goldstone modes. 4 2022. arXiv:2204.11629.

[3] Ian Low and Zhewei Yin. Soft Bootstrap and Effective Field Theories. *JHEP*, 11:078, 2019. arXiv:1904.12859, doi:10.1007/JHEP11(2019)078.

[4] Clifford Cheung, Karol Kampf, Jiri Novotny, Chia-Hsien Shen, and Jaroslav Trnka. A Periodic Table of Effective Field Theories. *JHEP*, 02:020, 2017. arXiv:1611.03137, doi:10.1007/JHEP02(2017)020.

[5] Clifford Cheung, Karol Kampf, Jiri Novotny, and Jaroslav Trnka. Effective Field Theories from Soft Limits of Scattering Amplitudes. *Phys. Rev. Lett.*, 114(22):221602, 2015. arXiv:1412.4095, doi:10.1103/PhysRevLett.114.221602.

[6] Garrett Goon, Scott Melville, and Johannes Noller. Quantum corrections to generic branes: DBI, NLSM, and more. *JHEP*, 01:159, 2021. arXiv:2010.05913, doi:10.1007/JHEP01(2021)159.

[7] Sam Veldmeijer. Extending the Double Copy for Scalar Effective Field Theories. URL: http://fse.studenttheses.ub.rug.nl/id/eprint/27319.

[8] H. Kawai, D.C. Lewellen, and S.-H.H. Tye. A relation between tree amplitudes of closed and open strings. *Nuclear Physics B*, 269(1):1–23, 1986. URL: https://www.sciencedirect.com/science/article/pii/0550321386903627, doi:https://doi.org/10.1016/0550-3213(86)90362-7.

[9] Clifford Cheung. *TASI Lectures on Scattering Amplitudes*, pages 571–623. 2018. arXiv:1708.03872, doi:10.1142/9789813233348_0008.

[10] Stephen L. Adler. Consistency conditions on the strong interactions implied by a partially conserved axial vector current. *Phys. Rev.*, 137:B1022–B1033, 1965. doi:10.1103/PhysRev.137.B1022.

[11] Steven Weinberg. Infrared photons and gravitons. *Phys. Rev.*, 140:B516–B524, 1965. doi:10.1103/PhysRev.140.B516.

[12] Johannes Broedel, Marius de Leeuw, Jan Plefka, and Matteo Rosso. Constraining subleading soft gluon and graviton theorems. *Phys. Rev. D*, 90(6):065024, 2014. arXiv:1406.6574, doi:10.1103/PhysRevD.90.065024.

[13] Freddy Cachazo, Song He, and Ellis Ye Yuan. New Double Soft Emission Theorems. *Phys. Rev. D*, 92(6):065030, 2015. arXiv:1503.04816, doi:10.1103/PhysRevD.92.065030.

[14] Ricardo Monteiro, Donal O'Connell, and Chris D. White. Black holes and the double copy. *JHEP*, 12:056, 2014. arXiv:1410.0239, doi:10.1007/JHEP12(2014)056.

[15] Andrés Luna, Ricardo Monteiro, Donal O'Connell, and Chris D. White. The classical double copy for Taub–NUT spacetime. *Phys. Lett. B*, 750:272–277, 2015. arXiv:1507.01869, doi:10.1016/j.physletb.2015.09.021.

[16] Andrés Luna Godoy. *The double copy and classical solutions*. PhD thesis, Glasgow U., 2018.

[17] Andrés Luna, Ricardo Monteiro, Isobel Nicholson, Donal O'Connell, and Chris D. White. The double copy: Bremsstrahlung and accelerating black holes. *JHEP*, 06:023, 2016. arXiv:1603.05737, doi:10.1007/JHEP06(2016)023.

[18] B. Ananthanarayan. Pions: the original Nambu–Goldstone bosons: An introduction and precision pion physics. *Eur. Phys. J. ST*, 231(2):91–102, 2022. doi:10.1140/epjs/s11734-022-00443-7.

[19] B. Ananthanarayan. Research News - Meson scattering at high precision. *Curr. Sci.*, 92:886–887, 2007. arXiv:physics/0703141.

[20] The Editors of Encyclopaedia Britannica. Encyclopedia Britannica article on Yukawa Hideki. 01 2022. URL: https://www.britannica.com/biography/Yukawa-Hideki.

[21] Yuta Hamada and Sotaro Sugishita. Soft pion theorem, asymptotic symmetry and new memory effect. *JHEP*, 11:203, 2017. arXiv:1709.05018, doi:10.1007/JHEP11(2017)203.

[22] Bart Horn, Lam Hui, and Xiao Xiao. Soft-Pion Theorems for Large Scale Structure. *JCAP*, 09:044, 2014. arXiv:1406.0842, doi:10.1088/1475-7516/2014/09/044.

[23] Kurt Hinterbichler, Lam Hui, and Justin Khoury. An Infinite Set of Ward Identities for Adiabatic Modes in Cosmology. *JCAP*, 01:039, 2014. arXiv:1304.5527, doi:10.1088/1475-7516/2014/01/039.

[24] José M. Martín-García. xAct: Efficient tensor computer algebra for the Wolfram Language. URL: http://www.xact.es/.

[25] Joshua Ellis. Tikz Feynman latex package for Feynman diagrams. URL: https://jpellis.me/projects/tikz-feynman/tikz-feynman/ARC.

[26] Clifford Cheung, Andreas Helset, and Julio Parra-Martinez. Geometric soft theorems. *JHEP*, 04:011, 2022. arXiv:2111.03045, doi:10.1007/JHEP04(2022)011.

[27] Clifford Cheung, Karol Kampf, Jiri Novotny, Chia-Hsien Shen, and Jaroslav Trnka. On-Shell Recursion Relations for Effective Field Theories. *Phys. Rev. Lett.*, 116(4):041601, 2016. arXiv:1509.03309, doi:10.1103/PhysRevLett.116.041601.

[28] Arif Mohd. A note on asymptotic symmetries and soft-photon theorem. *JHEP*, 02:060, 2015. arXiv:1412.5365, doi:10.1007/JHEP02(2015)060.

[29] Clifford Cheung and James Mangan. Covariant color-kinematics duality. *JHEP*, 11:069, 2021. arXiv:2108.02276, doi:10.1007/JHEP11(2021)069.

[30] Noah Bittermann and Austin Joyce. Soft limits of the wavefunction in exceptional scalar theories. 3 2022. arXiv:2203.05576.

[31] Zhewei Yin. The Infrared Structure of Exceptional Scalar Theories. *JHEP*, 03:158, 2019. arXiv:1810.07186, doi:10.1007/JHEP03(2019)158.

[32] B. L. Cerchiai and M. Trigiante. On Multifield Born and Born-Infeld Theories and their non-Abelian Generalizations. *JHEP*, 10:160, 2016. arXiv:1609.07399, doi:10.1007/JHEP10(2016)160.

[33] Claudia de Rham and Andrew J. Tolley. DBI and the Galileon reunited. *JCAP*, 05:015, 2010. arXiv:1003.5917, doi:10.1088/1475-7516/2010/05/015.

[34] Song He, Linghui Hou, Jintian Tian, and Yong Zhang. Kinematic numerators from the worldsheet: cubic trees from labelled trees. *JHEP*, 08:118, 2021. arXiv:2103.15810, doi:10.1007/JHEP08(2021)118.

[35] Tomáš Brauner and Haruki Watanabe. Spontaneous breaking of spacetime symmetries and the inverse Higgs effect. *Phys. Rev. D*, 89(8):085004, 2014. arXiv:1401.5596, doi:10.1103/PhysRevD.89.085004.

[36] Z. Bern, J. J. M. Carrasco, and Henrik Johansson. New Relations for Gauge-Theory Amplitudes. *Phys. Rev. D*, 78:085011, 2008. arXiv:0805.3993, doi:10.1103/PhysRevD.78.085011.

[37] Henriette Elvang and Yu-tin Huang. Scattering Amplitudes. 8 2013. arXiv:1308.1697.

[38] Freddy Cachazo, Song He, and Ellis Ye Yuan. Scattering Equations and Matrices: From Einstein To Yang-Mills, DBI and NLSM. *JHEP*, 07:149, 2015. arXiv:1412.3479, doi:10.1007/JHEP07(2015)149.

[39] Laurentiu Rodina. Uniqueness from gauge invariance and the Adler zero. *JHEP*, 09:084, 2019. arXiv:1612.06342, doi:10.1007/JHEP09(2019)084.

[40] Clifford Cheung, Chia-Hsien Shen, and Congkao Wen. Unifying Relations for Scattering Amplitudes. *JHEP*, 02:095, 2018. arXiv:1705.03025, doi:10.1007/JHEP02(2018)095.

[41] Tomáš Brauner and Haruki Watanabe. Spontaneous breaking of spacetime symmetries and the inverse Higgs effect. *Phys. Rev. D*, 89(8):085004, 2014. arXiv:1401.5596, doi:10.1103/PhysRevD.89.085004.

[42] P. V. Dong, L. T. Hue, H. T. Hung, H. N. Long, and N. H. Thao. Symmetry Factors of Feynman Diagrams for Scalar Fields. *Theor. Math. Phys.*, 165:1500–1511, 2010. arXiv:0907.0859, doi:10.1007/s11232-010-0124-1.

[43] Michael E. Peskin and Daniel V. Schroeder. *An Introduction to quantum field theory*. Addison-Wesley, Reading, USA, 1995.

[44] B. Ananthanarayan and Shayan Ghosh. Pion Interactions and the Standard Model at High Precision. 12 2018. arXiv:1901.11061.

[45] F. E. Low. Bremsstrahlung of very low-energy quanta in elementary particle collisions. *Phys. Rev.*, 110:974–977, 1958. doi:10.1103/PhysRev.110.974.

[46] Temple He, Vyacheslav Lysov, Prahar Mitra, and Andrew Strominger. BMS supertranslations and Weinberg's soft graviton theorem. *JHEP*, 05:151, 2015. arXiv:1401.7026, doi:10.1007/JHEP05(2015)151.

[47] David Tong. Lecture Notes on Quantum Field Theory. URL: https://www.damtp.cam.ac.uk/user/tong/qft.html.